Influence of Transverse Rotating Magnetic Field on Enhancement of Solid Dissolution Process

Rafał Rakoczy and Stanisław Masiuk
Institute of Chemical Engineering and Environmental Protection Processes, West Pomeranian University of Technology, Szczecin 71-065, Poland

DOI 10.1002/aic.12097
Published online October 29, 2009 in Wiley InterScience (www.interscience.wiley.com).

The main objective of this work is to study the effect of transverse rotating magnetic field (TRMF) on the enhancement of solid dissolution process in the novel type reactor (TRMFR). The application of magnetically driven fluidization (MDF with homogeneous and heterogeneous systems) on mass transfer process is presented. A study of the effect of ferromagnetic particles content on solid–liquid mass transfer has been made. The experimental investigations are provided for the explanation of the influence on the dissolution process of a solid body to surrounding its dilute solution in a novel type reactor with the ferromagnetic particles suspended. The mass transfer coefficient is calculated from a kinetic equation and correlated in the relationship including standard and magnetic dimensionless numbers. The overall enhancements due to TRMF and MDF were compared. Unique correlating relations were obtained to generalize the experimental database. © 2009 American Institute of Chemical Engineers *AIChE J,* 56: 1416–1433, 2010

Keywords: mass transfer, liquid–solid contacting operations, transverse rotating magnetic field (TRMF), magnetically driven fluidization (MDF)

Introduction

The design, scale-up, and optimization of chemical engineering processes conducted in typical mixers require the knowledge of the fluid behavior during the mass and heat transfer processes.[1] Studies of the effect of vibration on mass transfer in a gas liquid contradicting in a reciprocating plate column were considered.[2–9] The dissolution of solid particles into water and other solutions was investigated,[10] where vibratory agitation realized by using circular flat disc without perforation. The mass transfer coefficient is calculated by measuring the slope of the concentration time curve in the initial process of particle dissolution. The breakage of chalk aggregates in both the vibrating and rotating mixers and analyze of the model of breakage which relates the pseudo-equilibrium aggregate size to the energy dissipation rate in the agitated vessel has been investigated.[11] The mass transfer investigations have been carried out in a vertical tubular cylindrical vessel equipped with the different number of the perforated plates agitators.[12] The novel approach to the mixing process is based on the application of magnetic fields to produce better hydrodynamic conditions in the case of the mass transfer process.

Magnetically assisted fluidization (MAF) is widely encountered in practical applications and in manufacturing of drugs, food, chemical products, biochemistry, and many other fields of technology. From classical point of view, the fluidized bed is a two-phase system with an intensive movement of dispersed solids. The description of behavior of this system is determined by considering the balance of the forces acting upon particles, i.e., gravitational forces, fluid-particle drag forces, and friction forces between particles.[13,14] MAF is a technique combining classical fluidization with an externally applied magnetic field.[15] This type of the field (or electric, sound, vibrations, ultrasound) is often applied to control powder bed via external magnetic field.[16–18]

Correspondence concerning this article should be addressed to R. Rakoczy at rrakoczy@zut.edu.pl.

© 2009 American Institute of Chemical Engineers

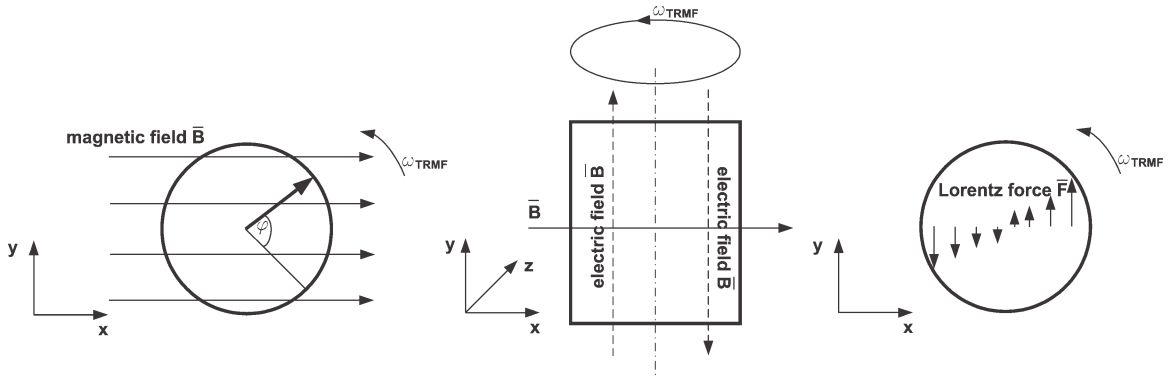

Figure 1. The effect of TRMF on the electrical conducting fluid.

This approach causes magnetically driven fluidization (MDF) in accordance with the classification.[19] The particles motions inside the fluidization volume are caused due to the space and time variable magnetic field driving the particles through a relatively stagnant fluid. The movement of particles may be controlled by means of the strong body magnetic forces. Beds of relatively large magnetic particle (beyond 15 vol %) exhibit effects of strong interparticle contacts and improved fluidization behavior in either of two basic magnetization modes, FIRST (the magnetic field act on he particles before applying flow) and LAST (the application of magnetic field to an already fluidized bed).[20] It is well known that the hydrodynamic behavior of magnetic fluidization has strong influence on the heat transfer and temperature distribution across the bed.[21,22]

MAF may be realized by using the DC or AC fields creating interparticles forces strong enough to provoke particles flocculation.[15] Moreover, studies over the recent decades were concerned with application of static, rotating, or alternating magnetic fields in different areas of engineering processes. Application of transverse rotating fields is a relatively new idea successfully applied to gas–liquid fluidization.[23–25] These experimental results reported that transverse rotating magnetic field (TRMF) may be considered as a significant improvement of MAF among the dominating experimental studies in axial fields. It is well known that the magnetic particles could form chains along the field lines.[26,27] The iron particles chains could rotate with the external rotating magnetic field in liquid–solid particles system. These particles can act as small agitators, shattering agglomerates and eliminating slugs and channels. From practical point of view, particles chains formation may be correlated as a function of magnetic field intensity, electric current frequency, and fraction of iron particles.[28] Compared to the static fields, rotating ones are distinguished by much lower energy consumption.

Many industrial applications rely on gas–solid fluidization to process their products due to its many advantages, such as good mixing or enhancement of heat and mass transfer rates. The movement of magnetic particles excited under TRMF improved the hydrodynamic conditions inside the fluidization vessel (lack of channels and fluid axial dispersion).[29] This movement may be controlled by field intensity and field orientation. Recent experiments have shown that the application of MDF to the mass transfer can significantly enhance this process.[30,31] The application of TRMF to a fluidized bed of ferromagnetic particles led to intensive magnetic stirring and improves mass transfer process.[32,33]

From the data available in technical literature, it is clear that the attention has not been focused on the mass transfer in the dissolution of a solid body to the surrounding liquid under action of MDF. From practical point of view, the dissolution process of solid particles is involved by means of the turbulently agitated systems[34] or ultrasound effect and chemical reaction.[35] In previous publications are no available data describing the mass transfer operations or the dissolution processes under MDF conditions induced by TRMF in a novel type of reactor. Therefore, the present work was aimed at systematically studying mass transfer in this type of transverse rotating magnetic field reactor (TRMFR) with a suspension of the ferromagnetic particles. Moreover, the influence of TRMF on the dissolution kinetics of the NaCl cylinder is presented. It is decided that in the present report, the influence of TRMF on the mass transfer enhancement is described using the non-dimensional parameters formulated on the base of fluid mechanics equations. These dimensionless numbers allow quantitative representation and characterization of the influence of hydrodynamic state under MDF conditions on the mass transfer process. The dimensionless groups are used to establish the effect of TRMF on this operation in the form of dimensionless correlations.

Transverse Rotating Magnetic Field

Recently, TRMF are widely used to control different processes in the various engineering operations. This kind of magnetic field induces a time-averaged azimuthal force, which drives the flow of the electrical conducting fluid in circumferential direction. The magnetic filed lines rotate in the horizontal direction with the rotation frequency of the field, $\overline{\omega}_{\mathrm{TRMF}}$. It is obvious that this parameter is equal to the frequency of alternating current. An electrical field, $\overline{E}$, is generated perpendicular to the magnetic field, $\overline{B}$. Perpendicular to the electric field, the Lorenz magnetic force, $\overline{F}_{\mathrm{m}}$, is acting as the driving force for the liquid rotation. The effect of TRMF on the electrical conducting fluid is graphically presented in Figure 1.

The TRMF may be generated by cylindrical inductor resembling the stator of a three-phase asynchronous electrical engine. The similar inductor of TRMF was

applied.[18,36,37] In the case of the electrical conducting fluid, the TRMF induces currents inside this liquid. These interact with the field of the inductor and generate electromagnetic force inside the electrical conducting liquid. The pattern of hydrodynamic flows due to TRMF in a cylindrical volume depends on the number of pole pair, p_{RMF}, of TRMF inductor. The distribution of TRMF may be considered as the quasi-uniform or non-uniform for the number of pole pair equal to 1 and $p_{\mathrm{RMF}} > 1$, respectively. The application of TRMF may generated the specific flow in a liquid cylindrical volume. The liquid flow is an azimuthal motion of medium around the central axis of the cylindrical volume. This flow is directed as the magnetic field rotates and the azimuthal velocity is maximal at the cylindrical vessel's walls. Obviously, this movement may determine the heat or mass transfer inside the rotating liquid.

Problem Formulation of Mass Diffusion Under the Action of Magnetic Field

In the case of these experimental investigations of mass transfer from solid body to its no flowing surrounding dilute solution, the boundary layer around the sample is generated. This layer around the sample is dispersed in the reactor volume by means of the physical diffusion processes and the diffusion due to TRMF. Then, the differential equation of mass balance equation for the mass concentration of component b, c_{b}, diffuses to the surrounding liquid phase may be given by:

$$\frac{\partial c_{\mathrm{b}}}{\partial \tau} + \mathrm{div}(c_{\mathrm{b}}\overline{w_{\mathrm{b}}}) + \mathrm{div}\left(\overline{j_{\mathrm{b}}}\right) + \mathrm{div}\frac{\overline{F_{\mathrm{m}}}}{\rho_w} = \frac{j_{\mathrm{b}}}{\rho_w} \tag{1}$$

The influence of TRMF on mass transfer process is manifested by the magnetic force defined as the divergence of Maxwell's stress tensor and expressed by:

$$\overline{F_{\mathrm{m}}} = \mathrm{div}\left[-\frac{1}{2}\mu_{\mathrm{m}}\overline{H}^2 E + \mu_{\mathrm{m}}\left(\overline{HH}\right)\right] = -\frac{1}{2\mu_{\mathrm{m}}}\mathrm{grad}\overline{B}^2 + \frac{1}{\mu_{\mathrm{m}}}\mathrm{Div}\left(\overline{BB}\right) \tag{2}$$

The magnetic pressure $\left(\frac{1}{2\mu_{\mathrm{m}}}\mathrm{grad}\overline{B}^2\right)$ has strong influence on the enhancement of diffusion process. In the above Eq. 2, the term $\left(\frac{1}{\mu_{\mathrm{m}}}\mathrm{Div}\left(\overline{BB}\right)\right)$ may be treated as the part of magnetic force and this expression describes the enhancement of flux density by the forced mass convection.

The velocity of component b, $\overline{w_{\mathrm{b}}}$, in relation to the motionless liquid phase may be treated as the convection velocity, whereas the term $\overline{j_{\mathrm{b}}}$ (see Eq. 1) is total diffusion flux density of component *b*. Taking into consideration of the intensification of the dissolution of solid body into liquid phase solution under the action of the rotating magnetic field, this density is functionally connected with the local thermodynamic state. The resulting diffusion flux is expressed as a sum of elementary fluxes considering the concentration, temperature, thermodynamic pressure gradients, and the pressure of magnetic field gradient in the following form:

$$\overline{j_{\mathrm{b}}} = \overline{j_{\mathrm{b}}}(\rho_{\mathrm{b}}) + \overline{j_{\mathrm{b}}}(T) + \overline{j_{\mathrm{b}}}(p) + \overline{j_{\mathrm{b}}}(p_{\mathrm{m}}) \tag{3}$$

According to the above Eq. 3, the particular components determines the molecular diffusion, $\bar{j}(\rho_i)$, the thermodiffusion, $\bar{j}(T)$, the barodiffusion, $\bar{j}(p)$, and the pressure of magnetic field gradient, $\bar{j}(p_{\mathrm{m}})$. Given the parameters of the thermodynamic state, Eq. 3 may be rewritten in the following form:

$$\overline{j_{\mathrm{b}}} = -D_{\mathrm{NaCl}}\,\mathrm{grad}\rho_{\mathrm{b}} - a_{\mathrm{b}}\left(\frac{\partial \rho_{\mathrm{b}}}{\partial T}\right)_{\substack{p=\mathrm{const}\\ p_{\mathrm{m}}=\mathrm{const}}}\mathrm{grad}T - v_{\mathrm{b}}\left(\frac{\partial \rho_{\mathrm{b}}}{\partial p}\right)_{\substack{T=\mathrm{const}\\ p_{\mathrm{m}}=\mathrm{const}}}\mathrm{grad}p - v_{\mathrm{m,b}}\left(\frac{\partial \rho_i}{\partial p_{\mathrm{m}}}\right)_{\substack{T=\mathrm{const}\\ p=\mathrm{const}}}\mathrm{grad}p_{\mathrm{m}} \tag{4}$$

Influence of Transverse Rotating Magnetic Field on Mass Transfer Process

As mentioned earlier, the experimental measurements of the influence of TRMF on the mass transfer process is described by the differential equation of mass balance equation for component *b* (see Eq. 1). Introducing the relations, Eqs. 2 and 4 in Eq. 1, gives the following relationship for the mass balance of *b* component:

$$\frac{\partial c_{\mathrm{b}}}{\partial \tau} + \mathrm{div}(c_{\mathrm{b}}\overline{w_{\mathrm{b}}}) + \mathrm{div}\left[-D_{\mathrm{NaCl}}\mathrm{grad}c_{\mathrm{b}} - a_{\mathrm{b}}\left(\frac{\partial c_{\mathrm{b}}}{\partial T}\right)_{\substack{p=\mathrm{const}\\ p_{\mathrm{m}}=\mathrm{const}}}\mathrm{grad}T - v_{\mathrm{b}}\left(\frac{\partial c_{\mathrm{b}}}{\partial p}\right)_{\substack{T=\mathrm{const}\\ p_{\mathrm{m}}=\mathrm{const}}}\mathrm{grad}p - v_{\mathrm{m.b}}\left(\frac{\partial c_{\mathrm{b}}}{\partial p_{\mathrm{m}}}\right)_{\substack{T=\mathrm{const}\\ p=\mathrm{const}}}\mathrm{grad}p_{\mathrm{m}}\right] + \mathrm{div}\left(\frac{d^2}{\rho_w v_{\mathrm{m,b}}\mu_{\mathrm{m,b}}}\mathrm{Div}\left(\overline{B}\,\overline{B}\right)\right) = \frac{j_b}{\rho_w} \tag{5}$$

The right side of the above Eq. 5 represents the source mass flux of component *b*. This expression may be represented by the differential kinetic equation for the dissolution of solid body as follows:

$$\beta_{\mathrm{NaCl}} = \frac{dm_{\mathrm{NaCl}}(\tau)}{F_{\mathrm{s}}(\tau)dc_{\mathrm{NaCl}}(\tau)d\tau} \tag{6}$$

Taking into account the above relationship (Eqs. 6 and 5), we obtain the following general relationship for the mass balance of component *b*:

$$\frac{\partial c_{\mathrm{b}}}{\partial \tau} + \mathrm{div}(c_{\mathrm{b}}\overline{w_{\mathrm{b}}}) + \mathrm{div}\left[-D_{\mathrm{NaCl}}\mathrm{grad}c_{\mathrm{b}} - a_{\mathrm{b}}\left(\frac{\partial c_{\mathrm{b}}}{\partial T}\right)_{\substack{p=\mathrm{const}\\ p_{\mathrm{m}}=\mathrm{const}}}\mathrm{grad}T - v_{\mathrm{b}}\left(\frac{\partial c_{\mathrm{b}}}{\partial p}\right)_{\substack{T=\mathrm{const}\\ p_{\mathrm{m}}=\mathrm{const}}}\mathrm{grad}p - v_{\mathrm{m.b}}\left(\frac{\partial c_{\mathrm{b}}}{\partial p_{\mathrm{m}}}\right)_{\substack{T=\mathrm{const}\\ p=\mathrm{const}}}\mathrm{grad}p_{\mathrm{m}}\right] + \mathrm{div}\left(\frac{d^2}{\rho_w v_{\mathrm{m,b}}\mu_{\mathrm{m,b}}}\mathrm{Div}\left(\overline{B}\,\overline{B}\right)\right) = -\frac{\beta_{\mathrm{NaCl}}\mathrm{grad}\,c_{\mathrm{b}}}{\rho_w} \tag{7}$$

The governing Eq. 7 may be rewritten in a symbolic shape which is useful for the dimensionless analysis. The

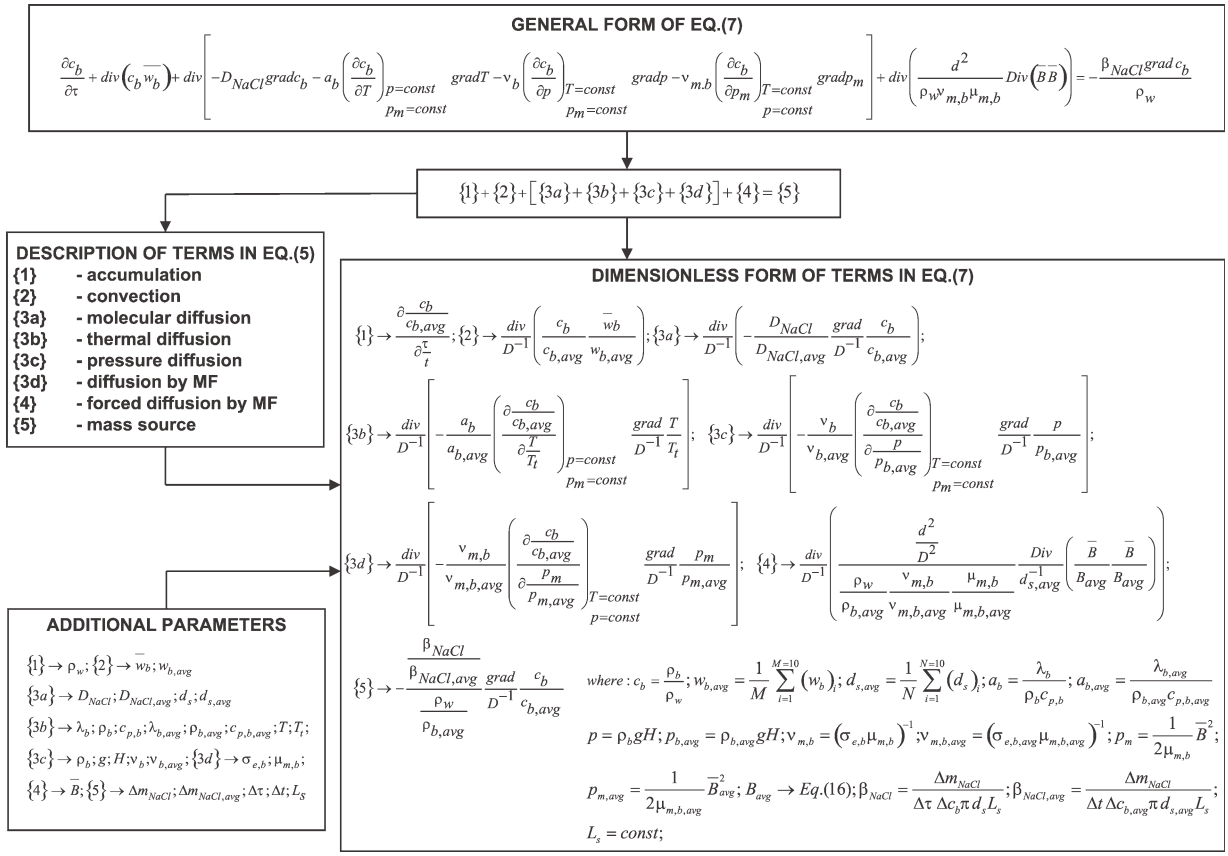

Figure 2. Graphical presentation of process calculation of dimensionless form of Eq. 7.

presentation of process calculation of the dimensionless form of Eq. 7 is graphically given in Figure 2.

The non-dimensional form of this equation may be scaled against the convective term. The creation of dimensionless numbers is also presented as diagram in Figure 3.

Taking into account the proposed diagrams (see Figures 2 and 3), we find the following dimensionless governing equation:

$$\frac{1}{S}\left[\frac{\partial c_b}{\partial \tau}\right]^* + \left[\mathrm{div}(c_b\overline{w_b})\right]^* + \left[-A_1 - B_1 - C_1 - D_1\right] + Ta_m\, Sc\left[\mathrm{div}\left(\frac{d^2}{\rho_w \nu_{m,b}\mu_{m,b}}\mathrm{Div}\left(\overline{B}\,\overline{B}\right)\right)\right]^* = -Sh\left[\frac{\beta_{NaCl}}{\rho_w}\mathrm{grad}c_b\right]^* \quad (8)$$

Dimensionless parameters appear in a natural way in Eq. 8 as ratios of corresponding terms. Table 1 shows the relationships of the parameters A_1, B_1, C_1, and D_1 in the form of Eqs. 9a–9d.

Moreover, Table 2 summarizes all essential and independent dimensionless parameters met in mass transfer process under the action of TRMF.

It is customary to introduce a dimensionless number called the magnetic Taylor number, Ta_m, to describe the convection due to the applied TRMF. This dimensionless number can also be described as the product of the squared Hartman number, as the acting force of the magnetic field, and the rotational Reynolds number. On the base of fluid mechanics equations for the electric and magnetic field, the dimensionless numbers has been established and it may be used to describe a flow phenomenon of electrical conducting liquid. In the presence of a steady or a rotating magnetic field, the relative influence of magnetic Lorentz forces vs. viscous forces is determined by means of the Hartman number. It should be noticed that the Hartman number is proportional to the strength of the produced magnetic field and its square is a measure of the relative importance of the electromagnetic to the viscous force. The strong magnetic field, corresponding to the large values of dimensionless Hartman number, $Ha > 1$. Moreover, the magnetic Reynolds number, Re_m, directly analogous to the normal Reynolds number, to describe the relative importance of flux freezing and diffusion. This dimensionless number measures the relative importance of advection and diffusion of magnetic field. When $Re_m >> 1$, the field lines are effectively frozen into the fluid and when $Re_m << 1$ dissipation is dominant.

Influence of Magnetic Driven Fluidization on Mass Transfer Process

In the case of the present study, ferromagnetic particles (Fe_3O_4) are fed into the working volume of reactor and suspended by means of the application of TRMF. Moreover, the state of ferromagnetic suspension may be achieved during the mass transfer process. A magnetic field changes the structure of the disperse system and generates eddies or

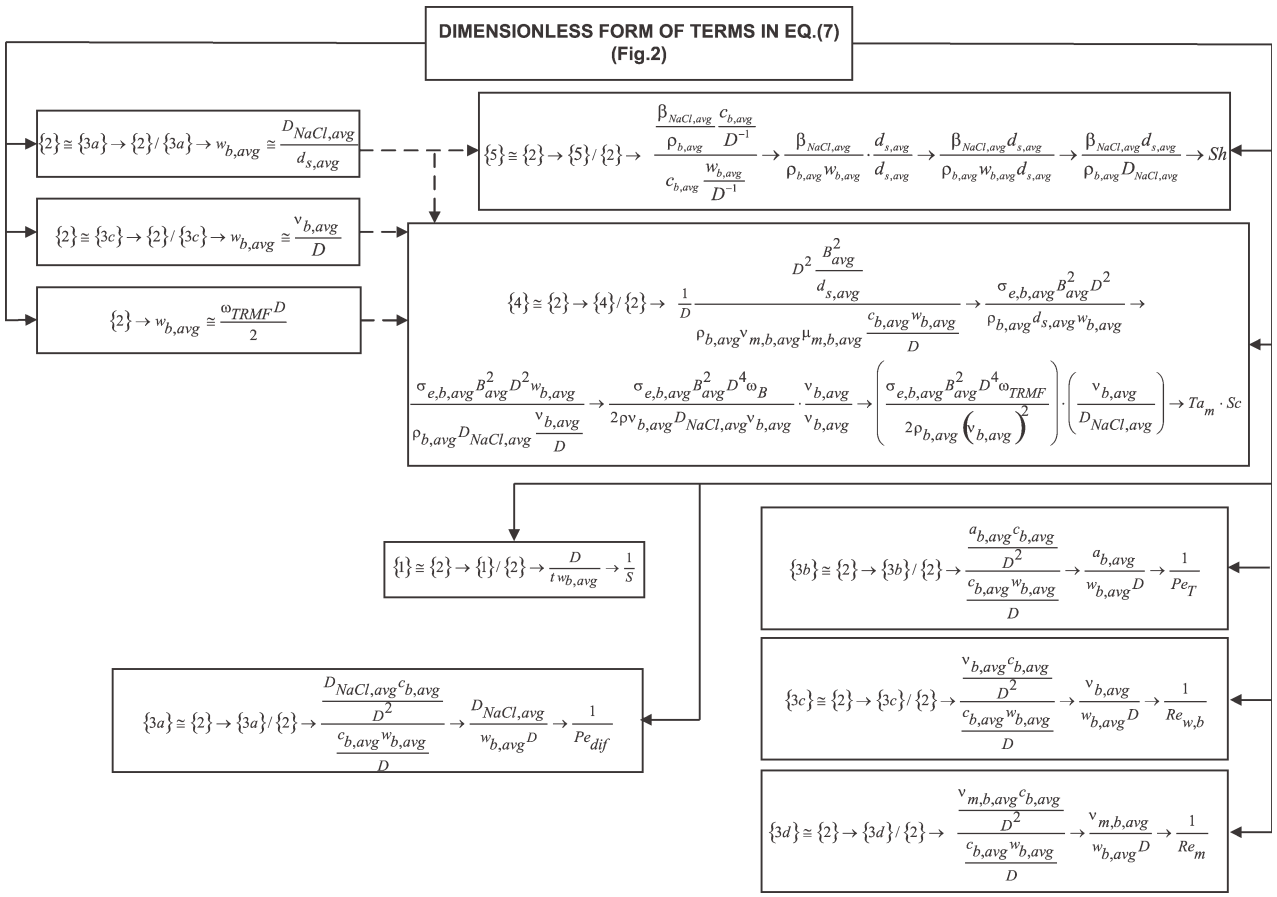

Figure 3. Definition of dimensionless numbers from Eq. 7.

microvortices in the surrounding liquid. It is well known that the ferromagnetic particles could form chains along the field lines and rotate with the external rotating magnetic field in the liquid-ferromagnetic particles mixture. Additionally, these particles may be treated as small agitators, involving the unsteady rotational movement of the reactor bulk. Thus, the application of ferromagnetic particles may improve the mass transfer process. The strong increase in mass transfer may be explained by the fact that the magnetic field energy is transformed to the movement of ferromagnetic particles. This resultant movement is connected with an increase in the relative velocity between the particle and surrounding medium. An increase in relative velocity leads to convective reduction of the boundary layer thickness around the solid body sample, and thus, to increase the mass transfer coefficient. Generally, the rotating frequency of the disperse system is equal to the frequency of alternating current. It should be noticed that the TRMF has non-homogenous field distributions of both the axial and radial field vector components. Therefore, the applied particles are distributed non-homogenously in the TRMFR volume.

It was decided that the mass transfer in the novel type of reactor (TRMFR) with the suspended ferromagnetic particles should be described by using the corrected form of Eq. 5.

The proposed expression is taken into consideration the rotational movement of ferromagnetic particles around the own axis and the axis of TRMFR. In this case, the general form of relation (5) may be rewritten as follows:

$$\frac{\partial c_{\mathrm{b}}}{\partial \tau}+\operatorname{div}\left(c_{\mathrm{b}}\overline{w_{\mathrm{b}}}\left(1+\frac{\overline{w_{\mathrm{b}}}}{w_{\mathrm{p}}}\right)\right)+\operatorname{div}\left[\begin{array}{l}-D_{\mathrm{NaCl}}\operatorname{grad}c_{\mathrm{b}}-a_{\mathrm{b}}\left(\dfrac{\partial c_{\mathrm{b}}}{\partial T}\right)_{\substack{p=\mathrm{const}\\ p_{\mathrm{m}}=\mathrm{const}}}\operatorname{grad}T \\ -v_{\mathrm{b}}\left(\dfrac{\partial c_{\mathrm{b}}}{\partial p}\right)_{\substack{T=\mathrm{const}\\ p_{\mathrm{m}}=\mathrm{const}}}\operatorname{grad}p-v_{\mathrm{m,b}}\left(\dfrac{\partial c_{\mathrm{b}}}{\partial p_{\mathrm{m}}}\right)_{\substack{T=\mathrm{const}\\ p=\mathrm{const}}}\operatorname{grad}p_{\mathrm{m}}\end{array}\right]$$
$$+\operatorname{div}\left(d^2\frac{\left(1+\frac{d_{\mathrm{p}}}{d}\right)}{\rho_w\, v_{\mathrm{m,b}}\,\mu_{\mathrm{m,b}}}\operatorname{Div}(\overline{B}\,\overline{B})\right)=-\frac{\beta_{\mathrm{NaCl}}}{\rho_w}\operatorname{grad}c_{\mathrm{b}} \quad (10)$$

Table 1. The Relationships Defined the Parameters A_1, B_1, C_1, and D_1 in Eq. 8

Parameter	Equation Number	Definition
A_1	(10a)	$\frac{1}{Pe_{\mathrm{dif}}}[\mathrm{div}(D_{\mathrm{NaCl}}\mathrm{grad}c_{\mathrm{b}})]^*$
B_1	(10b)	$\frac{1}{Pe_{\mathrm{T}}}\left[\mathrm{div}\left(a_{\mathrm{b}}\left(\frac{\partial c_{\mathrm{b}}}{\partial T}\right)_{\substack{p=\mathrm{const}\\ p_{\mathrm{m}}=\mathrm{const}}}\mathrm{gradT}\right)\right]^*$
C_1	(10c)	$\frac{1}{Re_{w,\mathrm{b}}}\left[\mathrm{div}\left(v_{\mathrm{b}}\left(\frac{\partial c_{\mathrm{b}}}{\partial p}\right)_{\substack{T=\mathrm{const}\\ p_{\mathrm{m}}=\mathrm{const}}}\mathrm{gradp}\right)\right]^*$
D_1	(10d)	$\frac{1}{Re_{\mathrm{m}}}\left[\mathrm{div}\left(v_{\mathrm{m,b}}\left(\frac{\partial c_{\mathrm{b}}}{\partial p_{\mathrm{m}}}\right)_{\substack{T=\mathrm{const}\\ p=\mathrm{const}}}\mathrm{gradp_m}\right)\right]^*$

Taking into account the relation (Eq. 10) and the definition of dimensionless numbers (see Figures 4 and 5) we find the following non-dimensional form of this equation:

$$\frac{1}{S}\left[\frac{\partial c_{\mathrm{b}}}{\partial \tau}\right]^* + \left[\mathrm{div}\left(c_{\mathrm{b}}\overline{w_{\mathrm{b}}}\left(1+\frac{\overline{w_{\mathrm{b}}}}{\overline{w_{\mathrm{p}}}}\right)\right)\right]^* + [-A_2 - B_2 - C_2 - D_2] + Ta_{\mathrm{m}}Sc\left(1+Re_{\omega,\mathrm{p}}\right)\left[\frac{D\left(1+\frac{d_{\mathrm{p}}}{D}\right)}{\rho_w v_{\mathrm{m,b}}\mu_{\mathrm{m,b}}}\mathrm{Div}\left(\overline{B}\,\overline{B}\right)\right]^* = -Sh\left(1+Re_{w,\mathrm{p}}\right)\left[\frac{\beta_{\mathrm{NaCl}}}{\rho_w}\mathrm{grad}c_{\mathrm{b}}\right]^* \quad (11)$$

As we see in Table 3, the definitions of parameters A_2, B_2, C_2, and D_2 (Eqs. 12a–12d) are presented.

An immediate consequence of these operations is that the application of magnetic particles may be characterized by parameters which are denoted as the rotational Reynolds number $Re_{\omega,\mathrm{p}}$ and the circular Reynolds number for ferromagnetic particles $Re_{w,\mathrm{p}}$. In the above Eq. 11, the rotational Reynolds number appears which is defined as follows:

$$Re_{\omega,\mathrm{p}} = \frac{\omega_{\mathrm{TRMF}} d_{\mathrm{p,avg}}^2}{v_{\mathrm{b,avg}}} \quad (13)$$

For description purposes, the circular Reynolds number for ferromagnetic particles was used, which includes the velocity of the particles as characteristic circular velocity. This dimensionless parameters can be determined according to the following definition:

$$Re_{w,\mathrm{p}} = \frac{w_{\mathrm{p,avg}} D}{v_{\mathrm{b,avg}}} \quad (14)$$

Principles of Transverse Rotating Magnetic Field Reactor

TRMF is often used instead of the mechanical mixing or may be added to convectional rotation mechanisms to augmentation of the chemical engineering processes. The stirring by RMF is schematically explained in Figure 6.

Table 2. Dimensionless Parameters in Eq. 8 and Their Physical Role

Name	Symbol	Definition	Significance	Remarks
Strouhal	S	$S = \frac{wt}{D}$	$\frac{\text{Convection}}{\text{Unsteadiness}}$	–
Péclet (mass)	Pe_{dif}	$Pe_{\mathrm{dif}} = Re\,Sc = \frac{wD}{D_{\mathrm{NaCl}}}$	$\frac{\text{Hydrodynamic convection}}{\text{Mass diffusion}}$	Re—Reynolds number Sc—Schmidt number
Péclet (heat)	Pe_{T}	$Pe_{\mathrm{T}} = Re\,Pr = \frac{wD}{a}$	$\frac{\text{Hydrodynamic convection}}{\text{Heat diffusion}}$	Pr—Prandtl number (is the ratio of the viscous and the therma diffusion and characterizes diffusive properties of fluid) $Pr = \frac{\text{momentum diffusion}}{\text{heat diffusion}}$
Reynolds	Re	$Re = \frac{wD}{v}$	$\frac{\text{Inertial force/convection}}{\text{Viscous force}}$	–
Magnetic reynolds	Re_{m}	$Re_{\mathrm{m}} = \frac{wD}{v_{\mathrm{m}}}$	$\frac{\text{Thermal diffusion}}{\text{Magnetic diffusion}}$	$Re_{\mathrm{m}} = \frac{Pr_{\mathrm{m}}}{Pr}$ pr_{m}—Magnetic Prandtl number (is the ratio of the viscous to the magnetic diffusion)
Sherwood	Sh	$Sh = \frac{k_{\mathrm{mass}} d_{\mathrm{s}}}{D_{\mathrm{NaCl}}}$	$\frac{\text{Convective mass transport}}{\text{Diffusive mass transport}}$	–
Schmidt	Sc	$Sc = \frac{v}{D_{\mathrm{NaCl}}}$	$\frac{\text{Momentum diffusion}}{\text{Molecular diffusion}}$	$Sc = \frac{Pe_{\mathrm{dif}}}{Re}$
Taylor	Ta	$Ta = \frac{\Omega_p^2 D^4}{v^2}$	$\frac{\text{centrifugal force}}{\text{viscous force}}$	$Ta_m = \frac{1}{2}\,Q\,Re_\omega = \frac{1}{2}\,Ha^2\,Re_\omega = \frac{\sigma_{\mathrm{e,b,avg}} B_{\mathrm{avg}}^2 D^4 \omega_{\mathrm{TRMF}}}{2\rho_{\mathrm{b,avg}}\left(v_{\mathrm{b,avg}}\right)^2}$ Magnetic Taylor number (describes the Lorenz-force amplitude of the rotating magnetic field) $Q = Ha^2 = \frac{\sigma_e D^2 B_0^2}{\rho v}$ Chandrasekhar number (is the ratio of the magnetic force to the dissipative force; is the square of the Hartmann number, Ha)

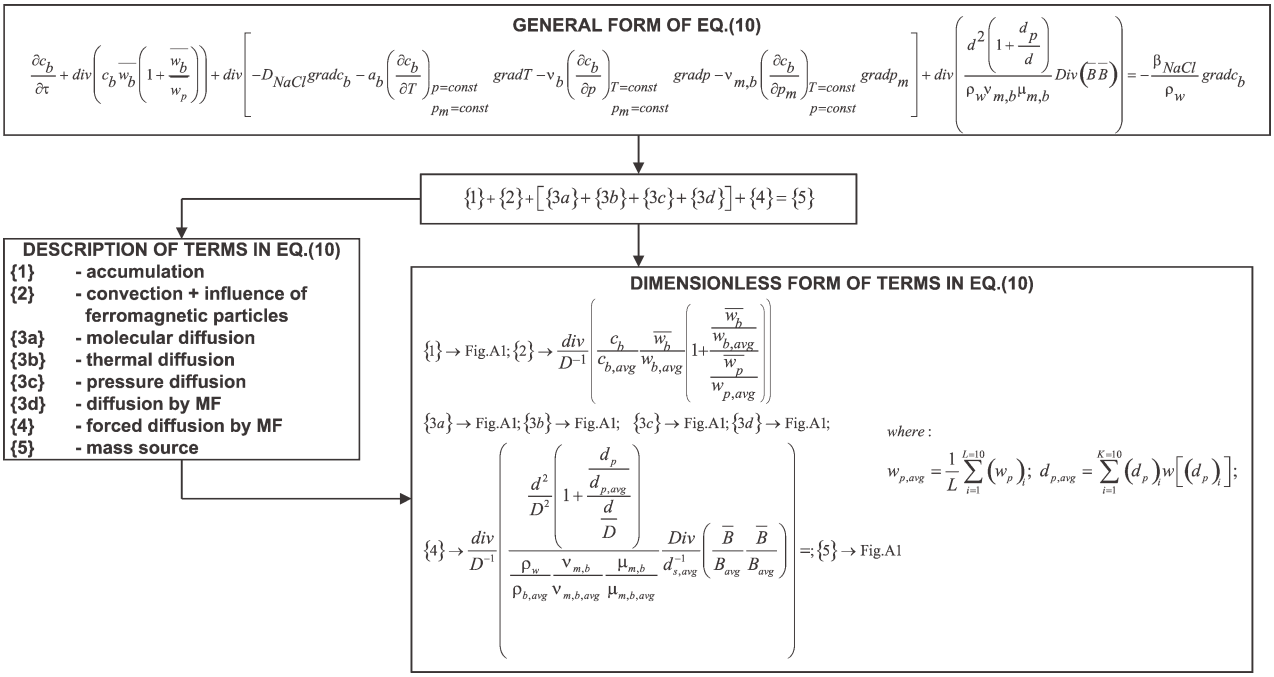

Figure 4. Graphical presentation of process calculation of dimensionless form of Eq. 10.

In the electrical conducting fluid, an arbitrary virtual loop is considered. When the electrical conductivity of liquid $\sigma_e \rightarrow \infty$, this loop rotates with the frequency equal to frequency of alternating current. According to the induction law, an electric current density, $\bar{j}_e$, is induced along the loop. The interaction between the current density and the magnetic

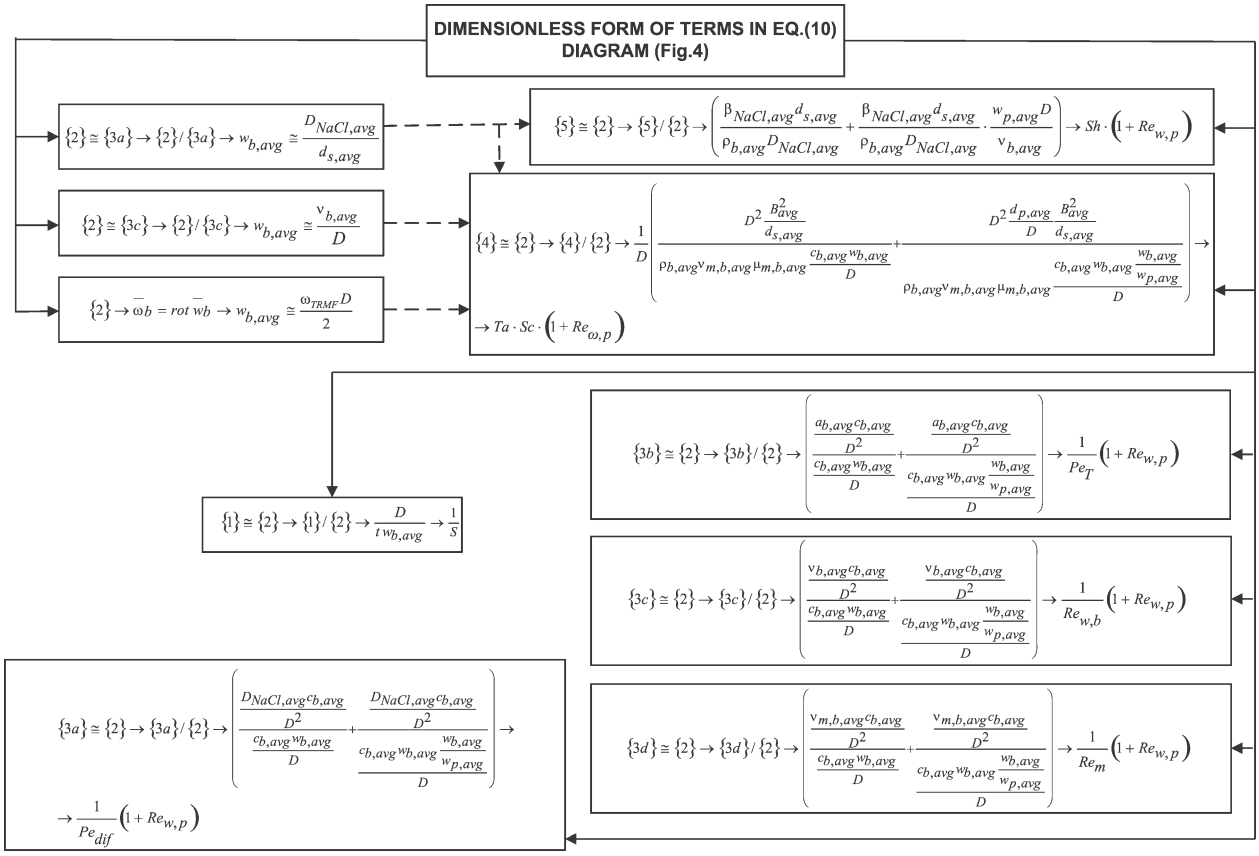

Figure 5. Definition of dimensionless numbers from Eq. 10.

Table 3. The Relationships Defined the Parameters A_2, B_2, C_2, and D_2 in Eq. 11

Parameter	Equation Number	Definition
A_2	(12a)	$\frac{1}{Pe_{\text{dif}}}\left(1+Re_{w,\text{p}}\right)[\text{div}D_{\text{NaCl}}\text{grad}c_{\text{b}}]^*$
B_2	(12b)	$\frac{1}{Pe_{\text{T}}}\left(1+Re_{w,\text{p}}\right)\left[\text{div}\left(a_{\text{b}}\left(\frac{\partial c_{\text{b}}}{\partial T}\right)_{\substack{p=\text{const}\\ p_{\text{m}}=\text{const}}}\text{grad}T\right)\right]^*$
C_2	(12c)	$\frac{1}{Re_{w,\text{b}}}\left(1+Re_{w,\text{p}}\right)\left[\text{div}\left(v_{\text{b}}\left(\frac{\partial c_{\text{b}}}{\partial p}\right)_{\substack{T=\text{const}\\ p_{\text{m}}=\text{const}}}\text{grad}p\right)\right]^*$
D_2	(12d)	$\frac{1}{Re_{\text{m}}}\left(1+Re_{w,\text{p}}\right)\left[\text{div}\left(v_{\text{m},b}\left(\frac{\partial c_{\text{b}}}{\partial p_{\text{m}}}\right)_{\substack{T=\text{const}\\ p_{\text{m}}=\text{const}}}\text{grad}p_{\text{m}}\right)\right]^*$

induction yields a volume force, $\overline{F}_{\text{m}}$, driving the liquid inside the cylindrical volume in the direction of the magnetic field rotation.

The impact of TRMF on suspended ferromagnetic particles, such as: Fe_3O_4, Fe_2O_3, or Fe powders may lead to a forced particle movement. The magnetic particles in a TRMF can display four kinds of motions, which include vibrating, forming rotating chains, moving around the vessel wall, and keeping still.[18] These particles may be fed into a reactor and suspended by the action of TRMF. Depending on the particle parameters, this may be achieved by a stirrer or, similar to a fluidized bed, by means of a flow.[32,33] In the case of this work, the process of dissolution of a solid body in a TRMF reactor was analyzed systematically using magnetic particles suspended in a stirred reactor. The suspended magnetic particles may be treated as the local micro-agitators. This kind of reactor is used in the biocatalitical reactor.[38,39]

Experimental Procedures

Experimental set-up

The all experimental measurements of the mass transfer process by using the rotating electromagnetic field were carried out on the basis of research in a laboratory set-up with the generator of electromagnetic field. A schematic of the experimental apparatus is presented in Figure 7.

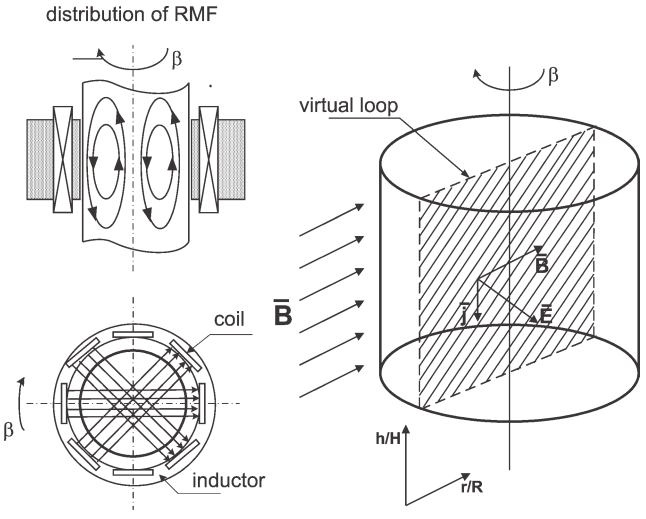

Figure 6. The graphical presentation of mixing with TRMF.

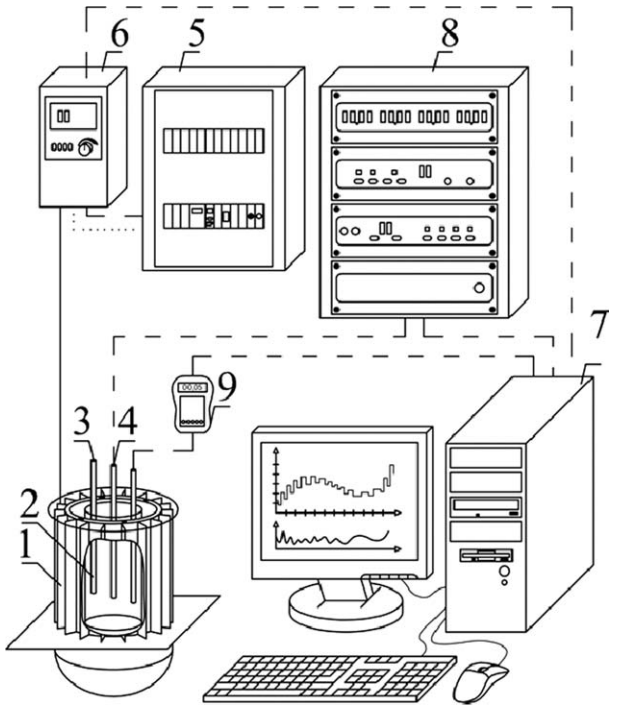

Figure 7. Sketch of experimental set-up: 1—generator of rotating magnetic field, 2—glass container, 3,4—conductivity probes, 5—electronic control box, 6—a.c. transistorized inverter, 7—personal computer, 8—multifunctional electronic switch, and 9—Hall probe.

This installation may be divided on the generator of the rotating electromagnetic field (1), glass container (2) with the conductivity probes (3–4), electric control box (5) and inverter (6) connected with multifunctional electronic switch (8) and the personal computer (7) equipped with the special software. This software was made possible to control the rotating electromagnetic field, the record of working parameters of generator, and the record of various state parameters. Main dimensions of the RMFR are given in Table 4.

As follows from the preliminary tests of the experimental apparatus, the glass container is not influenced on the working parameters of the stator.

TRMF was generated by means of the modified 3-phase stator of a induction squirrel-cage motor, which are compatible with Polish Standard PN-72/E-06000. The stator is supplied with 50 Hz three-phase alternating current. The transistorized inverter (4) was used to change the frequency of rotating magnetic field in the range of $f = 1$–50 Hz. The stator of electric machine, as the generator of RMF is made up of a number of stampings with slots to carry three phase winding. The number of pair poles per phase winding, p, is equal to 2. The windings are geometrically spaced 120° apart. The stator and the operating liquid may be treated as an apparent electrical circuit closed to the flux of magnetic induction. The stator windings are connected through a.c. transistorized inverter to the power source. The generator

Table 4. Dimensions of TRMF and Parameters of Ferromagnetic Particles

TRMF and Operating Conditions	Operating Range
Dimensions of TRMFR	
Inner diameter, m	0.015
Height, m	0.03
Height of liquid in container, m	0.019
Total volume, m^3	0.0053
Working volume, m^3	0.0034
Distance between the sides of container and the grooves of RMFR stator, m	0.001
Ferromagnetic particles	
Material	Fe_3O_4
Saturation magnetic moment, emu g^{-1}	87.1
Diameters for homogeneous system, m	1×10^{-3}; 1.5×10^{-3}; 2×10^{-3}
Mean diameter for heterogeneous system, m	0.5×10^{-3}
Particle density, kg m^{-3}	5810
Magnetic particle content, $kg_{Fe_3O_4}\ kg_{solvent}^{-1}$	0.003; 0.006; 0.012

produces an azimuthal electromagnetic force in the bulk of the RMF reactor with the magnetic field lines rotated in the horizontal plane.

Range of experimental investigations

The average mass transfer coefficient was calculated from a mass balance between a dissolving solid cylindrical sample and no flowing surrounding dilute solution. Two conductive probes connected to a multifunction computer meter were used to measuring and recording of the concentration of the achieve solution of the salt in the liquid bulk (distilled water). The mass of the rock salt sample decreasing during the process of dissolution is determined by a high sensitive electronic balance that connected with rocking double-arm lever. On the lever arm, the sample was hanging, the other arm connected to the balance. In the present investigation, the change in mass of solid body in a short time period of dissolution is very small and the surface of dissolved cylinder of the rock salt is insignificantly varied at the time. Then, the mean mass transfer coefficient may be calculated from the linear kinetics equation using the mean concentration driving force of the process determined from two time response curves. The range of experimental investigations is graphically presented in Figure 8.

The stirred bulk of the TRMFR was made of Fe_3O_4 particles (see Table 4). The impact of external alternating magnetic field on suspended ferromagnetic particles may led to a forced, very intensive particle movement. In case this experimental work, the influence of suspended ferromagnetic particles (homogeneous and heterogeneous systems) on mass transfer process is presented. Experimental measurements were performed for different diameter of ferromagnetic particles (d = 1 mm; 1.5 mm; 2 mm). Moreover, the effect of heterogeneous system of ferromagnetic particles on the mass transfer operation under the action of TRMF was analyzed (see histogram in Figure 8). The particle size analysis was determined by means of the projection microscope and the separate fractions were obtained by sieving. The analysis of the asymmetry and the kurtosis for the produced distribution

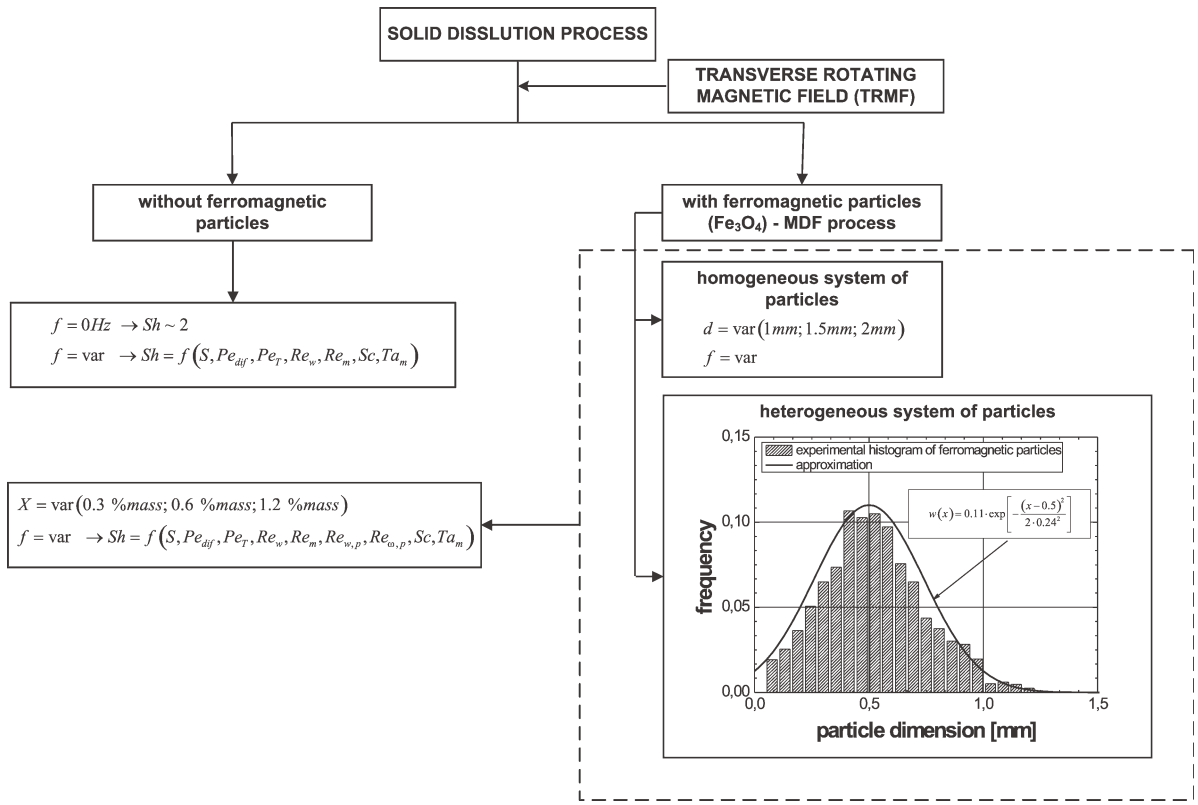

Figure 8. The graphical presentation of the range of experimental investigations.

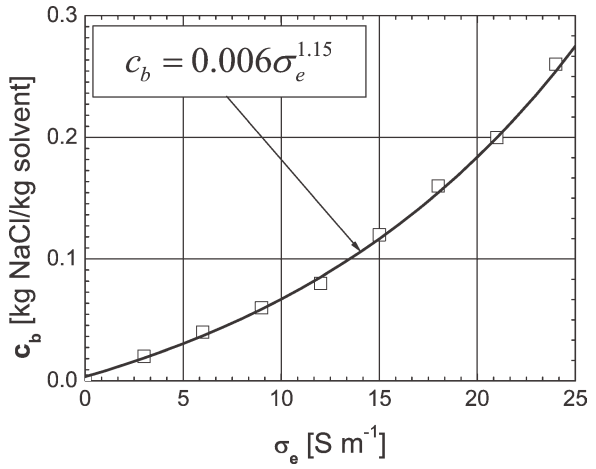

Figure 9. Calibration curve of the relative mass concentration of NaCl in relation with the electrical conductivity.

showed that the values of these numerical characteristic were mainly located in the intervals corresponding to the normal distribution (see relationship in Figure 8). From practical point of view, this system of ferromagnetic particles may be described by using the mean diameter. The value of this diameter for the analyzed case is equal to 0.5 mm.

Rock-salt sample

Raw rock-salt (>98% NaCl and rest traces quantitative of chloride of K, Ca, Mg, and insoluble mineral impurities) cylinders were not fit directly for the experiments because their structure was not homogeneous (certain porosity). Basic requirement concerning the experiments was creating possibly homogeneous transport conditions of mass on whole interfacial surface, which was the active surface of the solid body. These requirements were met thanks to proper preparing of the sample, mounting it in the mixer and matching proper time of dissolving. As an evident effect were fast showing big pinholes on the surface of the dissolved sample as results of local non-homogeneous of material. Departure from the shape of a simple geometrical body made it impossible to take measurements of its area with sufficient precision. So, it was necessary to put those samples through the process of so-called hardening. The turned cylinders had been soaked in saturated brine solution for about 15 min and than dried in a room temperature. This process was repeated four times. To help mount the sample in the mixer, a thin copper thread was glued into the sample's axis. The processing was finished with additional smoothing of the surface with fine-grained abrasive paper. A sample prepared in this way had been keeping its shape during dissolving for about 30 min. The duration of a run was usually 30 s. The rate of mass transfer involved did not produce significant dimensional change in diameter of the cylinder. The time of a single dissolving cycle was chosen so that the measurement of mass loss could be made with sufficient accuracy and the decrease of dimensions would be relatively small (maximum about 0.5 mm). Before starting every experiment, a sample whose height, diameter, and mass had been known was mounted in a mixer under the free surface of the mixed liquid. The generator of RMF started the recording of concentration changes in time, the weight showing changes in sample's mass during the process of solution, and time measuring was started simultaneously. After finishing the cycle of dissolving, the generator was stopped, and then, the loss of mass had been read on electronic scale and concentration of NaCl (electrical conductivity) in the mixer as well. This connection is given by a calibration curve, showing the dependence of the relative mass concentration of NaCl on the electrical conductivity (see Figure 9).

Patterns of magnetic induction

In the case of these experimental measurements, TRMF is generated by coils located around the cylinder, and the axes are directed along the radius. When the alternate current supplied the windings, the generated magnetic field rotates about the cylinder axis with the constant angular frequency ω_{TRMF}. The gaps between the electromagnet poles and the cylindrical column are minimal. An a.c. transistorized inverter controlled the rotating frequency (it is equal to the frequency of alternating current). A transformer that adjusted the alternating current fed to the stator coils controlled TRMF. The relationship between frequency of alternating current and current intensity is graphically presented in Figure 10. In the experiment, the rotating frequency is in the range of f = 1–50 Hz.

TRMF with the magnetic induction, B, is controlled by means of the a.c. alternating current frequency equal to the frequency of RMF. The values of magnetic induction at different points inside the cylindrical glass container are detected by using the Hall probe connected with the personal computer. On the basis of the records of magnetic induction random signals, the mean values of parameter, B, at each sampling point was calculated. As follows from the analysis of the experimental data, the values of magnetic induction are spatially distributed and independent at the time. It is seen that in the area occupied with this container, the RMF distribution depends strongly on the spatial coordinates (see Figure 11).

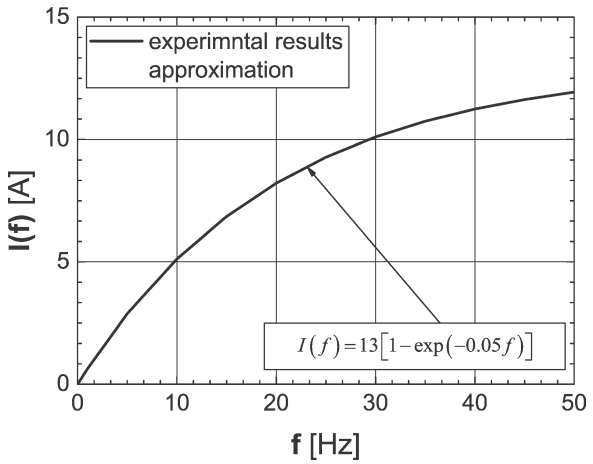

Figure 10. The relationship between frequency of alternating current and current intensity.

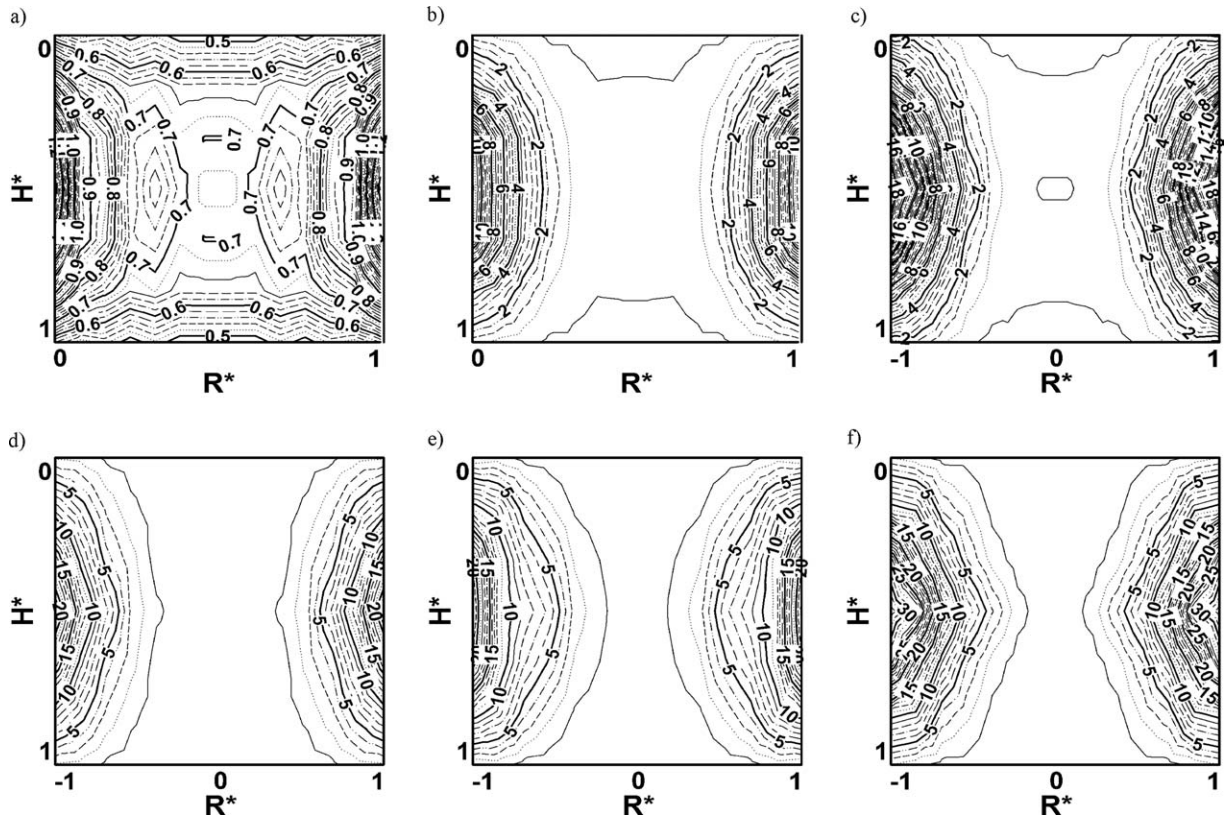

Figure 11. The typical contour patterns of spatial distribution of magnetic induction in the cross-section of the glass container.

(a) $f = 1$ Hz ($I(f) \cong \sim 0.65$ A), (b) $f = 10$ Hz ($I(f) \cong 5$ A), (c) $f = 20$ Hz ($I(f) \cong 8$ A), (d) $f = 30$ Hz ($I(f) \cong 10$ A), (e) $f = 40$ Hz ($I(f) \cong 11$A), and (f) $f = 50$ Hz ($I(f) \cong 12$ A).

Therefore, the experimentally observed effect of TRMF distribution should be mathematically described by means of the following equation in the system of coordinates $\left(H^* = {}^{h}/_{\boldsymbol{H}}; R^* = {}^{r}/_{R}\right)$:

$$B(H^*, R^*, I(f)) = p_1(R^*, I(f)) \exp\left[-0.5\left(\frac{H^* - 0.5}{p_2(R^*, I(f))}\right)^2\right] \tag{15}$$

The coefficients $p_1(R^*, I(f))$ and $p_2(R^*, I(f))$ are described by combination of three parameters depending on the current intensity as follows:

$$p_1(R^*, I(f)) = p_{11}(I(f))(R^*)^2 + p_{12}(I(f))R^* + p_{13}(I(f)) \tag{16a}$$

$$p_2(R^*, I(f)) = p_{21}(I(f)) + p_{22}(I(f)) \exp\left[-0.5\left(\frac{R^* - 0.5}{p_{23}(I(f))}\right)^2\right] \tag{16b}$$

Table 5 shows the relationships of the parameters in Eqs. 16a and 16b.

Considering the proposed analytical description, the contours of magnetic field for the various values of the alternating current frequency or current intensity may be obtained. Figures 12a, b show the distribution of TRMF from the experimental measurements and the proposed mathematical description, respectively.

The difference between the predicted and measured values of magnetic induction is less than $\pm 15\%$ for $\sim 80\%$ of the data points. On the basis of the analytical description of RMF distribution at different values of the current intensity, the averaged values of magnetic field may be calculated by double integration of the spatial distribution of this magnetic field parameter, as follows:

$$\left[B_{\text{avg}}\right]_{I(f)=\text{const}} = \int_{H^*} \int_{R^*} [B(H^*, R^*)]_{I(f)=\text{const}} \, dR^* \, dH^* \tag{17}$$

Table 5. The Relationships Defined the Parameters in Eqs. 16a and 16b

Parameter	Relation
$p_{11}(R^*, I(f))$	$2.84(I(f))^{1.54}$
$p_{12}(R^*, I(f))$	$-2.84(I(f))^{1.54}$
$p_{13}(R^*, I(f))$	$1.53(I(f))^{1.21}$
$p_{21}(R^*, I(f))$	$0.0023(I(f)) + 0.21$
$p_{22}(R^*, I(f))$	$0.45\exp(-0.16I(f))$
$p_{23}(R^*, I(f))$	$0.0013(I(f)) + 0.43$

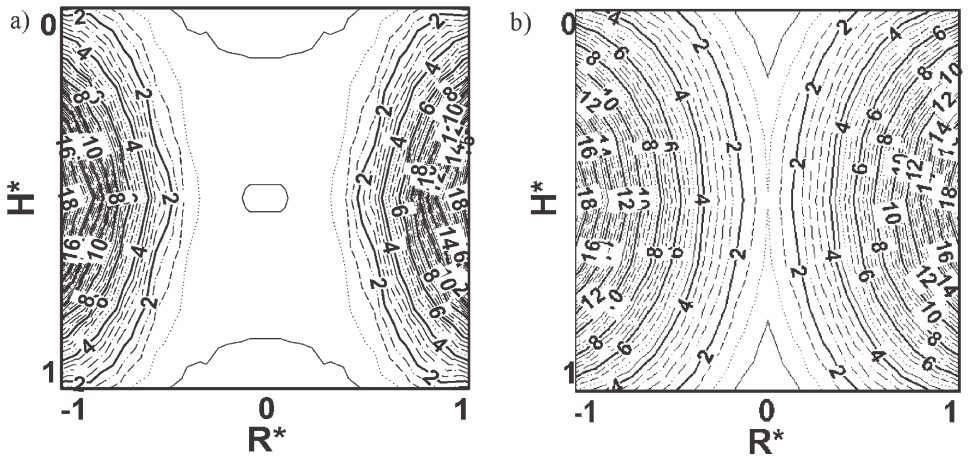

Figure 12. Comparison of TRMF distribution (f = 20 Hz ($I(f) \cong$ 8 A)) for the experimental measurements (a) and the proposed mathematical description (b).

The above Eq. 17 was solved by using the Matlab software. To establish the effect of the current intensity on the averaged value of magnetic field, the obtained data are graphically illustrated in Figure 13.

As follows from this figure, the scatter of the calculated data represented by points is strictly described by the proposed relationship with the averaged percentage error equal to 5%. The proposed description of magnetic induction is simple, effective, and accessible for engineering design with the application of TRMF because it employs standard mathematical methods and allows describing the spatial distribution of magnetic induction by the deterministic averaged analytical relationships.

Calculation of mass transfer coefficient

The mass transfer coefficient in a mixing process was calculated from a mass balance between a dissolving cylinder and its surrounding solution using Eq. 6. The integration of Eq. 6 is difficult because the area of solid body is strongly depended on the time of dissolving process. As mentioned earlier, the mean surface of cylinder may be used in Eq. 6. The driving force of mass transfer process, $dc_{\mathrm{NaCl}}(\tau)$, is calculated from two time response curves as the arithmetic mean, Δc_{NaCl}. On the basis of the accurate experimental data, the relation between loss of mass, mean area of mass transfer, and mean driving force of this process for the time of dissolving duration, Δt, is approximately linear and then the mass transfer coefficient may be calculated from the simple linear equation in the following form:

$$\beta_{\mathrm{NaCl,avg}} = \frac{\Delta m_{\mathrm{NaCl}}}{\pi d_{\mathrm{s,avg}} L_{\mathrm{s}} \Delta c_{\mathrm{NaCl}} \Delta t} \tag{18}$$

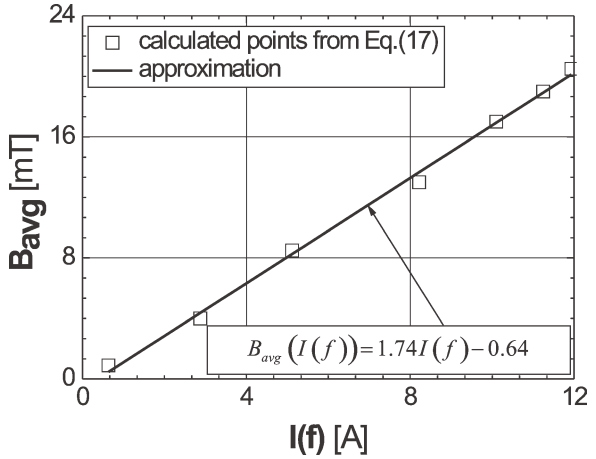

Figure 13. The graphical presentation of the relation between the current intensity and the averaged value of magnetic induction.

Results and Discussion

The equations that are predicted in this report in comparison to the very useful dimensionless relationships given in the prevent literature are much more attractive because it generalizes the experimental data in a relatively simple and uniform manner and valid for the wide range of the operating conditions. The all equations obtained in this report are valid for the operating parameters given in Table 6.

It is assumed, that the results of mass transfer experiments for the TRMFR should be correlated using the general form of the relationships obtained for the standard mixer devices.

Table 6. The Range of Operating Conditions

Parameter	Operating Range
Mean diameter of sample, m	0.023–0.031
Length of sample, m	0.071
Time of dissolution, s	30
Loss of mass for 30 s dissolution, kg	0.00014–0.015
Mean driving force, kg_{NaCl} kg^{-1}	0.0018–0.012
Frequency of TRMF, s^{-1}	1–50
Pulsation of TRMF, rad s^{-1}	6.28–314
Averaged magnetic induction, mT	0.6–12
Schmidt number	733–918
Sherwood number	2–285
Magnetic Taylor number	2×10^{-6}–0.5
Rotational Reynolds number	0.72–310

These equations have different form than that commonly proposed in the relevant literature.

It is decided that in the present report the mass transfer is described by the similar somewhat modified relationship between the dimensionless Sherwood number, Sh, and the numbers, which defined the intensity of magnetic effects in the tested TRMFR. Under TRMF conditions, a relationship for the mass transfer may be expressed in the following form:

$$Sh = fn_1\left(S, Pe_{\mathrm{dif}}, Pe_{\mathrm{T}}, Re_{w,\mathrm{b}}, Re_{\mathrm{m}}, Ta_{\mathrm{m}}, Sc\right) \tag{19}$$

Under MDF conditions, where the influence of particles movement is important, this expression becomes:

$$Sh = fn_2\left(S, Pe_{\mathrm{dif}}, Pe_{\mathrm{T}}, Re_{w}, Re_{\mathrm{m}}, Re_{w,\mathrm{p}}, Re_{\omega,\mathrm{p}}, Ta_{\mathrm{m}}, Sc\right) \tag{20}$$

For mass transfer under the action of TRMF and MDF realized in this experimental investigation, where $S, Pe_{\mathrm{dif}}, Pe_{\mathrm{T}}, Re_{w}, Re_{\mathrm{m}}$ numbers are practically invariable, the above expressions (20) reduce to

$$Sh = fn_3\left(Re_{w,\mathrm{p}}, Re_{\omega,\mathrm{p}}, Ta_{\mathrm{m}}, Sc\right) \tag{21}$$

Mass transfer process in the analyzed systems is very complicated and may be described by the non-dimensional Sherwood number, as a rule is a function of the Schmidt number and the dimensionless numbers describing the influence of TRMF and MDF on the realized process. Use of the dimensionless Sherwood number as a function of the various non-dimensional parameters (see Eq. 19) yields a description of liquid-side mass transfer, which is more general and useful. In majority of the works, both theoretical and practical, the correlations of mass transfer process without the magnetic field have the general form:

$$Sh = aRe^{b}Sc^{c} \tag{22}$$

where the Sherwood number is a function of the particle Reynolds number, the Schmidt number, and differ by the fitting parameters a, b, and c.

To establish the effect of TRMF and MDF on mass transfer enhancement in the novel type of TRMFR in the wide range of variables data obtained in the present work has been analyzed to propose the following relationship:

$$Sh = 2 + a\left[Ta_{\mathrm{m}}\left(\frac{1+Re_{\omega,\mathrm{p}}}{1+Re_{w,\mathrm{p}}}\right)\right]^{b} Sc^{c} \tag{23}$$

The general variation of mass transfer process under the action of TRMF or in the case of the controlled MDF process is non-well defined, and so, it seems that the proposed expression (see Eq. 23) may be used to generalize the experimental data. It was decided that the mass transfer in the novel type of TRMFR with the suspended ferromagnetic particles should be described by using the special correction term, $\left(\frac{1+Re_{\omega,\mathrm{p}}}{1+Re_{w,\mathrm{p}}}\right)$. The proposed expression (see Eq. 23) is taken into consideration the rotational and circular movement of ferromagnetic particles. On the base of the theoretical consideration (see chapter 3, Eq. 11), the form of correction term is established and it is included into the general relationship (23).

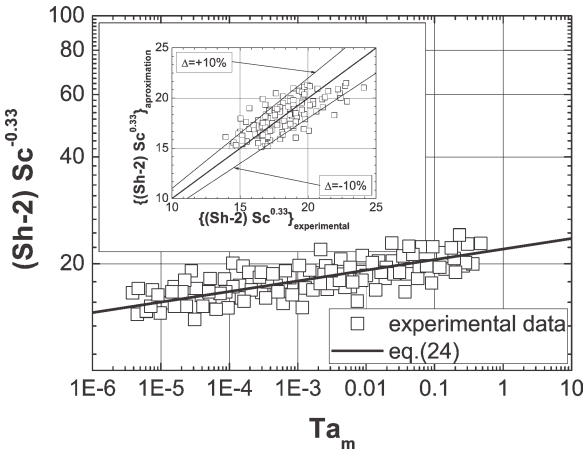

Figure 14. The graphical presentation of mass transfer data at TRMF.

Mass transfer from the solute into the surrounding liquid occurs in three ways. In an infinite stagnant liquid, mass transfer is involved by molecular diffusion augmented by the gradients of temperature and pressure. The natural convection current are set up owing to the difference in density between the pure solvent and the solution. This difference in induced flow helps to carry solute away from the interface. The third mode of transport is depended on the external effects. In this way, the forced convection closely resembles natural convection expect that the liquid flow is involved by using the external force. The limiting value of the dimensionless mass transfer Sherwood number is equal to 2. The obtained value of mass transfer by molecular diffusion is assigned to the Sherwood number at $Ta_{\mathrm{m}} = 0$, $Re_{\omega,\mathrm{p}} = 0$, and $Re_{w,\mathrm{p}} = 0$.

To establish the effect of mass transfer on the set of dimensionless parameters can be described by the variable $(Sh-2)Sc^{-c}$ proportional to term $a\left[Ta_{\mathrm{m}}\left(\frac{1+Re_{\omega,\mathrm{p}}}{1+Re_{w,\mathrm{p}}}\right)\right]^{b}$. The dimensionless groups were calculated with the physical properties at the mean bulk relative mass concentration in the temperature range of 20–25°C.

Effect of TRMF on mass transfer is indicated in Figure 14. The experimental results form the present study plotted in this figure in log–log system in the coordinates $((Sh-2)Sc^{-0.33}, Ta_{\mathrm{m}})$. In the case of this work, the experimental data have been correlated using the new modified dimensionless equation including Sherwood number as a ratio of the Schmidt and Taylor numbers. The exponent upon of the dimensionless Schmidt number is to be 0.33 as there is some theoretical and experimental evidence for this value. The experimental results in Figure 14 suggest that the term $(Sh-2)Sc^{-0.33}$ vs. the magnetic Taylor number may be analytically described by a unique monotonic function. These results for the whole range of the magnetic Taylor number can be approximated by using the software Matlab. A

straight line was drown through the points, representing the following relationship:

$$Sh = 2 + 22 \cdot Ta^{0.03} Sc^{0.33} \tag{24}$$

where the term $\left(\frac{1+Re_{\omega,\mathrm{p}}}{1+Re_{w,\mathrm{p}}}\right)$ is equal to 1 because the dimensionless Reynolds numbers, $Re_{\omega,\mathrm{p}}$ and $Re_{w,\mathrm{p}}$, are equal to 0, respectively.

In the left upper corner of Figure 14 is included the graphical presentation of comparison of the predicted values of dimensionless Sherwood number and the experimental results. Equation 24 predicts the mass transfer process within $\pm 10\%$. Moreover, for the proposed empirical correlation, the ranges of validity for Eq. 24 are collected in Table 6.

As can be clearly seen (see Figure 14) mass transfer rates, expressed as $(Sh-2)Sc^{-0.33}$, increase with increasing the averaged value of the magnetic induction. It was found that as the intensity of the magnetic field increases, the relative velocity of liquid inside the cylindrical container increases. The liquid rotation may be completely characterized by a single parameter which is denoted as the magnetic Taylor number. Moreover, this dimensionless number describes the Lorenz-force amplitude of the TRMF action and is a measure of azimuthal fluid velocity induced by this type of magnetic field. Equation 24 indicates that the mass transfer rates would increase with the magnetic Taylor number $Sh \sim Ta_{\mathrm{m}}^{0.03}$.

To study the influence of particle rotation induced by using TRMF on the dissolution process, the ferromagnetic (Fe_3O_4) particles were used. It is obvious that the mass transfer of suspended particles in a standard mixer or in TRMFR depends decisively on the suspension state. All experimental measurements were initiated by loading into glass container the magnetic particles (Fe_3O_4) with the mean diameters equal to 1 mm, 1.5 mm, and 2 mm for the homogeneous system particles. The separate fractions were obtained by sieving. In contrast to these particles, the heterogeneous system was used (see histogram in Figure 8). As follows from the analysis of the obtained histograms, the mean diameter of particles is equal to 0.5 mm.

Under the action of TRMF, the ferromagnetic particles are lifted and the disperse system behavior by increasing the magnetic field intensity may be observed. At the initial state of process production of disperse systems, the various fraction of ferromagnetic particles was put into a glass container with dispersing liquid, where the fraction was suspended by means of TRMF $\left(X = 0.003\frac{\mathrm{kg_{Fe_3O_4}}}{\mathrm{kg_{solvent}}};\ 0.006\frac{\mathrm{kg_{Fe_3O_4}}}{\mathrm{kg_{solvent}}};\ 0.012\frac{\mathrm{kg_{Fe_3O_4}}}{\mathrm{kg_{solvent}}}\right)$. In this work, the generalization of the experimental results of the dissolution process with MDF may be correlated by using Eq. 23. The proposed correlation shows proportionality between $(Sh-2)Sc^{-0.33}$ and $a\left[Ta_{\mathrm{m}}\left(\frac{1+Re_{\omega,\mathrm{p}}}{1+Re_{w,\mathrm{p}}}\right)\right]^b$ in which $Re_{\omega,\mathrm{p}}$ (Eq. 13) and $Re_{w,\mathrm{p}}$ (Eq. 14) describe the rotational and circular movement of the ferromagnetic particles. In the present work, where the dissolution process under the action of TRMF and MDF is considered, the value of curricular velocity of ferromagnetic particles, $w_{\mathrm{p,avg}}$, inside the cylindrical glass container is necessary to define. This velocity determines the mass transfer and it is very difficult to calculate. A good approximation may be obtained by introducing the liquid velocity $\left(w_{\mathrm{p,avg}} \approx 2w_{\mathrm{b,avg}} = \omega_{\mathrm{TRMF}} D\right)$ with the assumption

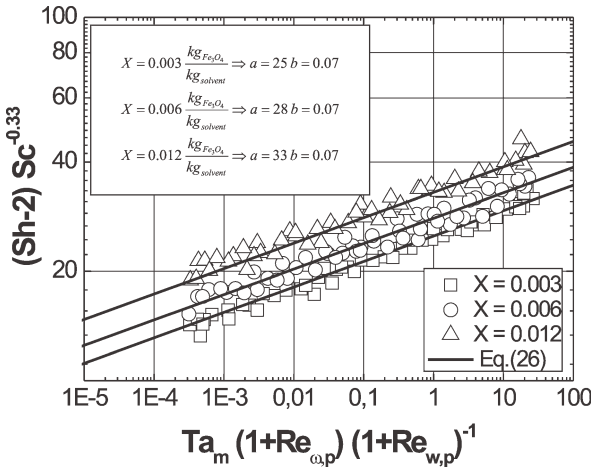

Figure 15. The graphical presentation of the influence of ferromagnetic particles content, *X*, on the mass transfer for the homogeneous particles system.

that the velocity particles are approximately equal to the adequate liquid velocity under the action of TRMF. It should be noticed that the enhancement of mass transfer rate is a result of a reduced laminar boundary layer thickness. The thickness of this layer decreases with increasing relative velocity between the liquid and the ferromagnetic particles.

Effect of ferromagnetic particles content, X, on the mass transfer is evolved by showing values $(Sh-2)Sc^{-0.33}$ against $\left[Ta_{\mathrm{m}}\left(\frac{1+Re_{\omega,\mathrm{p}}}{1+Re_{w,\mathrm{p}}}\right)\right]$ in Figure 15.

The experimental results shown in this figure suggest the following expression:

$$\frac{(Sh-2)}{Sc^{0.33}} = fn\left[Ta_{\mathrm{m}}\left(\frac{1+Re_{\omega,\mathrm{p}}}{1+Re_{w,\mathrm{p}}}\right), X\right] \tag{25}$$

where the Sherwood number is function of the adequate dimensionless numbers and the ferromagnetic particles content, X, for the homogeneous particles system. As follows from Figure 15, the scatter of experimental data represented by points is placed along the parallel straight lines. Therefore, the effect of ferromagnetic particles content for the homogeneous particles system may be described by means of the relatively simple unique dimensionless relationship as follows:

$$Sh = 2 + a\left[Ta_{\mathrm{m}}\left(\frac{1+Re_{\omega,\mathrm{p}}}{1+Re_{w,\mathrm{p}}}\right)\right]^b Sc^c X^d \tag{26}$$

The constant a and exponent b, c, and d in Eq. 26 are computed by using the principle of least square. Applying the software Matlab the analytical relationship may be obtained:

$$Sh = 2 + 76.5\left[Ta_{\mathrm{m}}\left(\frac{1+Re_{\omega,\mathrm{p}}}{1+Re_{w,\mathrm{p}}}\right)\right]^{0.07} Sc^{0.33} X^{0.2} \tag{27}$$

The graphical presentation of Eq. 27 is given in Figure 16.

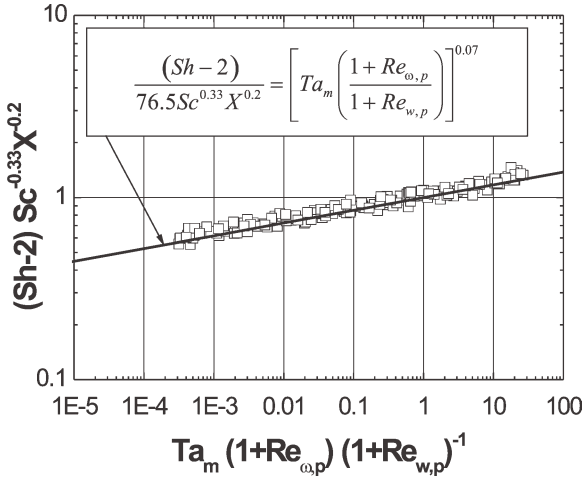

Figure 16. The graphical presentation of mass transfer data for the homogeneous particles system.

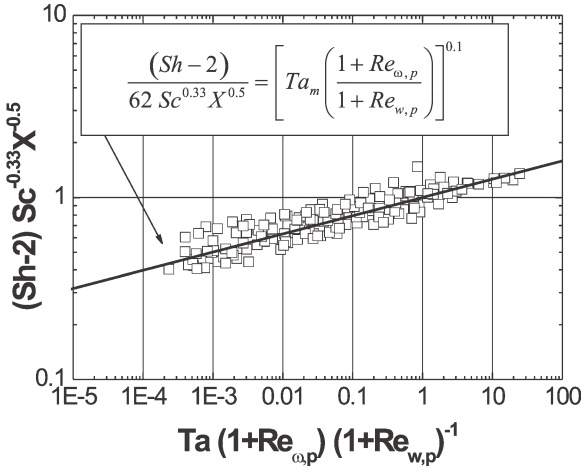

Figure 17. The graphical presentation of the influence of ferromagnetic particles content, *X*, on the mass transfer for the heterogeneous particles system.

The proposed form of Eq. 27, which is presented in Figure 16 as the full curve, correlates the data very well with a standard deviation $\sigma = 0.0148$. The average percentage error of all the data is $+0.0236\%$. The difference between the predicted and measured values is less than $\pm 10\%$ for $\sim 80\%$ of the data points. Figure 16 demonstrate that, within the limits of scatter among the plotted data represented by the points, the mass transfer rate (dimensionless Sherwood number) increase with increasing the term $a\left[Ta_{\mathrm{m}}\left(\frac{1+Re_{\omega,\mathrm{p}}}{1+Re_{w,\mathrm{p}}}\right)\right]^{b} Sc^{c}X^{d}$. This figure shows a strong increase in mass transfer process when the ferromagnetic particles are applied. It was found that the Sherwood number increase with increase in the magnetic Taylor number. According to the action of MDF, these particles generate the local micro-vortices in the whole volume of liquid and the rotational Reynolds, $Re_{\omega,\mathrm{p}}$, and the curricular Reynolds, $Re_{w,\mathrm{p}}$, numbers increases. It should be noted that the mass transfer rate is increased with the ferromagnetic particles content as $X^{0.2}$.

Mass transfer experiments were also performed either for heterogeneous particles system (see histogram in Figure 8). Under the influence of the motion of ferromagnetic particles in the TRMF, the eddies or macrovortices that decompose into increasingly smaller vortices in a cascade-like manner until a microscale is reached. The heterogeneous particles system may cause the high efficiency of magnetic mixing and it leads to an increase in the relative velocity between the particles and the surrounding medium.

The influence of heterogeneous particles system on the mass transfer rates, expressed as $(Sh-2)Sc^{-0.33}$, is graphically presented in Figure 17.

Forced mass transfer under the action of MDF with the heterogeneous particles system may be conveniently correlated by using the proposed expression (25). The relationship between the variables in this equation has been established from experimental measurements given in Figure 17. Experiments were also performed by changing the ferromagnetic particles content, *X*. The experimental results presented in Figure 17 suggest that the mass transfer process may be analytically described by a unique monotonic function (25). Applying the software Matlab the analytical relationship are correlated in the lines proposed in this Figure 17.

The influence of ferromagnetic particles content on the mass transfer rates may also be expressed by means of the equation similar to relation (26):

$$Sh = 2 + 62\left[Ta_{\mathrm{m}}\left(\frac{1+Re_{\omega,\mathrm{p}}}{1+Re_{w,\mathrm{p}}}\right)\right]^{0.1} Sc^{0.33}X^{0.5} \qquad (28)$$

The obtained results may be graphically presented in Figure 18. It should be noted that the mass transfer rate in this case is increased with the ferromagnetic particles content as $X^{0.5}$. The regression analysis of the data yielded the proposed relationship (see in Figure 18) with the standard deviation $\sigma = 0.0293$ and with the averaged relative error $\pm 18\%$.

The experimental investigations of the influence of magnetic field on the dissolution process were performed at various conditions (TRMF, MDF with homogeneous particles

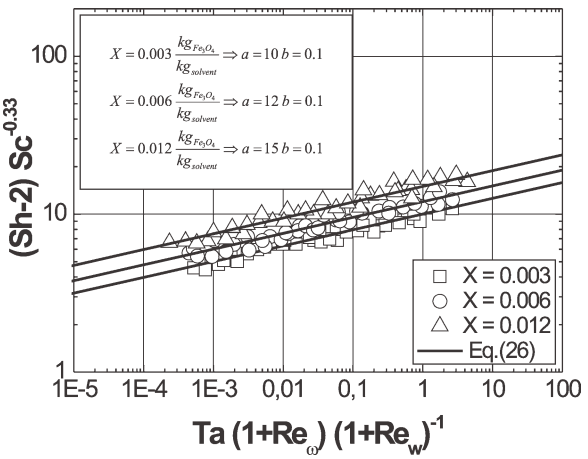

Figure 18. The graphical presentation of mass transfer data for the heterogeneous particles system.

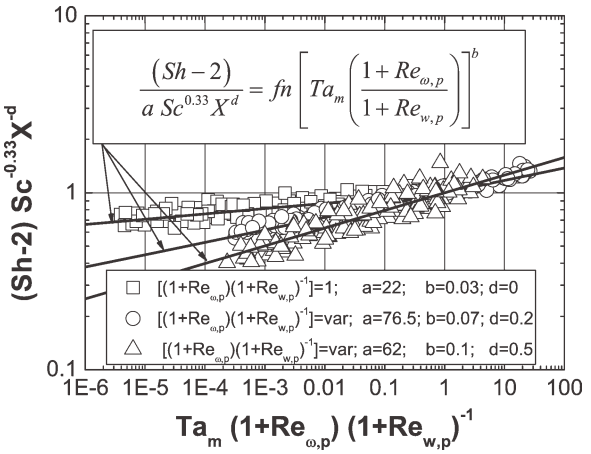

Figure 19. Comparison of experimental results for various augmentation technique (TRMF, MDF with homogeneous particles system, MDF with heterogeneous particles system).

system, MDF with heterogeneous particles system). It is clear that the effect of magnetic field on the mass process is depended on the augmentation technique. Comparison of the obtained results for this technique is graphically shown in Figure 19.

The mass transfer data are drawn in Figure 19 with $\left(\frac{(Sh-2)}{Sc^{0.33}X^{d}}\right)$ as a function of term $\left[Ta_{\mathrm{m}}\left(\frac{1+Re_{\omega,\mathrm{p}}}{1+Re_{w,\mathrm{p}}}\right)\right]^{b}$. It is indicated in the plots that the mass transfer ratio as module $\left[Ta_{\mathrm{m}}\left(\frac{1+Re_{\omega,\mathrm{p}}}{1+Re_{w,\mathrm{p}}}\right)\right]^{b}$ is increased from 4×10^{-5} to 34. The plots also confirm that the augmentation technique has significant effect on mass transfer process. The main aim of the presented experimental investigation was shown the influence of various augmentation technique connected with the magnetic field on mass transfer process. The appropriate conclusion should be received from the comparison of values of term $\left(\frac{(Sh-2)}{Sc^{0.33}X^{d}}\right)$ for the analyzed stages. This comparison is graphically presented in Figure 19. On the basis of the observations of the curve paths in Figure 19, three stages can be identified:

Stage I

$$-\left(4\cdot 10^{-5} \le \left[Ta_{\mathrm{m}}(1+Re_{\omega,\mathrm{p}})(1+Re_{w,\mathrm{p}})^{-1}\right]^{b} < 0.1\right),$$

Stage II

$$-\left(0.1 \le \left[Ta_{\mathrm{m}}(1+Re_{\omega,\mathrm{p}})(1+Re_{w,\mathrm{p}})^{-1}\right]^{b} < 5\right),$$

Stage III

$$-\left(5 \le \left[Ta_{\mathrm{m}}(1+Re_{\omega,\mathrm{p}})(1+Re_{w,\mathrm{p}})^{-1}\right]^{b} < 34\right),$$

In Stage I, the mass transfer rate is found to increase with increase in applied magnetic field. Moreover, Figure 19 shows a strong increase in mass transfer process when the ferromagnetic particles is not applied. For homogeneous and heterogeneous particles systems, initially, there is pronounced increase of mass transfer rates in dependence of term $\left[Ta_{\mathrm{m}}\left(\frac{1+Re_{\omega,\mathrm{p}}}{1+Re_{w,\mathrm{p}}}\right)\right]^{b}$. Further increase of the magnetic field intensity leads to even higher mass transfer rates, however, the slope is much upper than in the first stage. The high efficiency of TRMF for the lower value of magnetic field in Stage I may be explained by the fact that movement energy is directly transferred to the liquid. When the TRMF rotated slowly, the ferromagnetic particles may be treated as small agitators mixing the liquid near the wall of the cylindrical container. Moreover, the NaCl-cylinder was placed in the middle of TRMFR. Compared to TRMFR with suspended ferromagnetic particles, TRMF at small values of magnetic induction caused the mass transfer to be enhanced by up to 40%. It is obvious that the mass transfer rate should increase with increasing particle rotation frequency. Improvements in this process may be realized by considering the synergic effect of TRMF and ferromagnetic particles. In Stage II, the mass transfer process augments with an increase in frequency of TRMF and magnetic field intensity. It should be noticed, that the ferromagnetic particles content is a very important parameter. The experimental data are correlated by fixing the exponent value of 0.2 and 0.5 on the homogeneous and heterogeneous particles systems, respectively. When the TRMF rotated faster (stage III), the resulting ferromagnetic particles movement directly leads to an increase in the relative velocity particles and the surrounding liquid medium. The effect of magnetically induced particle rotation is described by means of the rotational Reynolds number. Moreover, the curricular Reynolds provides a possibility to characterize a liquid movement. It is interesting to note that the influence of heterogeneous particles system on the mass transfer rate is higher than in the case of the homogeneous particles system. As follows from these considerations, the magnetic field may be successfully applied for the enhancement of mass transfer rate. Additionally, the influence of MDF on this process was studied systematically using the homogeneous and heterogeneous particles systems. In this article, the obtained experimental data were generalized using the new form of equation in which the influence of magnetic parameters on the dissolution process was established. The proposed general relationship (see Eq. 25) turned out to be a suitable description for characterizing the influence of TRMF and MDF on the mass transfer process. The proposed empirical correlations derived allows to predict the experimentally determined dimensionless Sherwood numbers well over the wide range of the operating parameters.

Conclusions

The present experimental study shows interesting features concerning the effects of TRMF and MDF on the mass transfer process. Inspecting the obtained measurements reveals the following conclusions.

1. The study of magnetic field effects on the solid of nearly constant geometry enables the focus to be on the mass transfer process. TRMF and MDF results in significant enhancement of the solid dissolution rate. The mass transfer rate in the presence of magnetic field and the suspended ferromagnetic particles indicated strong dependency on the magnetic induction.

2. The TRMF and MDF have different influence on the mass transfer rate. For TRMF, the mass transfer rate increases with an increase in magnetic field intensity. It was found that the TRMF strongly influenced on the mass transfer process. This process is improved by means of the ferromagnetic particles suspended in a bulk of TRMFR.

3. With respect to the other very useful mass transfer equations given in the pertinent literature, the theoretical description of problem and the equations predicted in the present article is much more attractive because it generalizes the experimental data taking into consideration the various parameters, which defined the hydrodynamic state and the intensity of magnetic effects in the tested TRMFR.

4. On the basis of the experimental investigations, the results were successfully correlated by using the general relationship (26). Enhancement of magnetic field to the mass transfer rate may be described by this proposed equation. Further studies of both theoretical and experimental nature are required to optimize the effects of TRMF or MDF on the mass transfer process as well as to understand the mechanism of enhancement.

Notation

a = thermal diffuses m^2s^{-1}
$\overline{B}$ = magnetic induction vector $kgA^{-1}s^{-2}$
c_p = heat capacity $Jkg^{-1}K^{-1}$
c_b = relative mass concentration $kg_{NaCl}kg^{-1}$
d_p = ferromagnetic particle diameter m
d_s = sample diameter m
D = diameter of container m
D_{Nacl} = diffusion coefficient m^2s^{-1}
f = frequency of electrical current s^{-1}
F_s = cylindrical surface of dissoluble sample m^2
$\overline{H}$ = magnetic field strength vector Am^{-1}
$H[m]$ = liquid level in glass container m
$\overline{j_b}$ = mass flux vector $kg_{NaCl}mkg^{-1}s^{-1}$
$\overline{j}$ = electrical current density vector Am^{-2}
j = volumetric mass source $kg_{NaCl}m^{-3}s^{-1}$
L_s = length of sample m
m_{Nacl} = mass of dissoluble NaCl sample kg_{Nacl}
p = hydrodynamic pressure Nm^{-2}
p_m = magnetic pressure Nm^{-2}
R = radius of glass container m
t = time s
T = temperature °C
$\overline{w_b}$ = vector of brine circular velocity ms^{-1}
$\overline{w_p}$ = vector of ferromagnetic particle circular velocity ms^{-1}

Greek letters

β_{Nacl} = mass transfer coefficient $kg_{NaCl}m^{-2}s^{-1}$
λ = thermal conductivity $Jm^{-1}s^{-1}K^{-1}$
μ_m = magnetic permeability $kgmA^{-2}s^{-2}$
ν = kinematic viscosity, m^2s^{-1}
ν_m = magnetic viscosity, m^2s^{-1}
ρ = density $kgm^{-3}$$
σ_e = electrical conductivity $A^2s^3kg^{-1}m^{-3}$
τ = time dissolution s
ω_B = angular velocity of magnetic field rad s^{-1}

Dimensionless numbers

Ha = Hartman number –
Pe_{dif} = diffusion Peclet number –
Pe_T = thermal Peclet number –
Re_m = magnetic Reynolds number –
$Re_{w,b}$ = fluid circular Reynolds number –
$Re_{\omega,b}$ = particle rotational Reynolds number –
S = Strouhal number –
Sc = Schmidt number –
Sh = Sherwood number –
Ta_m = magnetic Taylor number –

Subscripts

avg = average
b = brine
e = electrical
dif = diffusion
m = magnetic
p = particle
s = sample
w = circular velocity
ω = angular velocity
* = dimensionless

Abbreviations

AC = alternating current
DC = direct current
MAF = magnetically assisted fluidization
MF = magnetic field
MDF = magnetically driven fluidization
TRMF = transverse rotating magnetic field
TRMFR = transverse rotating magnetic field reactor

Literature Cited

1. Zlokarnik M. *Stirring: Theory and Practice*. Weinheim: WileyVCH, 2001.
2. Gomaa HG, Landau J, Al-Taweel AM. Gas–liquid contacting in reciprocating plate columns. I. Hydrodynamics. *Can J Chem Eng*. 1991;69:228–239.
3. Sundaresan A, Varma YBG. Interfacial area and mass transfer in gas–liquid cocurrent upflow and countercurrent flow in reciprocating plate column. *Can J Chem Eng*. 1990;68:952–988.
4. Rama Rao NV, Baird MHI. Characteristics of a counter current reciprocating plate bubble column. I. Holdup, pressure drop and bubble diameter. *Can J Chem Eng*. 1998;66:211–221.
5. Baird MHI, Rama Rao NV. Characteristics of a counter current reciprocating plate bubble column. II. Axial mixing and mass transfer. *Can J Chem Eng*. 1988;66:222–230.
6. Rama Rao NV, Baird MHI. Gas liquid mass transfer in a 15 cm diameter reciprocating plate column. *J Chem Technol Biotechnol*. 2003;78:134–137.
7. Rama Rao NV, Baird MHI. Axial mixing and gas holdup with reciprocating doughnut plates. *Can J Chem Eng*. 2000;78:261–264.
8. Baird MHI, Rama Rao NV, Vijayan S. Axial mixing and mass transfer in a vibrating perforated plate extraction column. *Can J Chem Eng*. 1992;70:69–76.
9. Gomaa HG, Al-Taweel AM. Axial mixing in a novel pilot scale gas–liquid reciprocating plate column. *Chem Eng Process*. 2005;44:1285–1295.
10. Tojo K, Miyanami K, Minami I. Vibartory agitation in solid-liquid mixing. *Chem Eng Sci*. 1981;36:279–284.
11. Shamlou PA, Gierczycki AT, Tichner-Hooker NJ. Breakage of flocs in liquid suspensions agitated by vibrating and rotating mixers. *Chem Eng J*. 1996;62:23–34.
12. Masiuk S, Rakoczy R. Power consumption, mixing time, heat and mass transfer measurements for liquid vessels that are mixed using reciprocating multiplates agitators. *Chem Eng Process*. 2007;46:89–98.
13. Yates JG. *Fundamentals of Fluidized-Bed Chemical Processes*. London: Butterworths, 1983.
14. Hristov JY. Fluidization of ferromagnetic particles in a magnetic field. Part 2: Field effects on preliminary gas fluidized bed. *Powder Technol*. 1998;97:35–44.
15. Hristov JY, Fachikov L. An overview of separation by magnetically stabilized beds: state-of-the-art and potential applications. *China Particuology*. 2007;5:11–18.

16. Zeng P, Zhou T, Yang J. Behavior of mixtures of nano-particles in magnetically assisted fluidized bed. *Chem Eng Process: Process Intens.* 2008;47:101–108.
17. Yang J, Sliva A, Banerjee A, Dave RN, Pfeffer R. Dry particle coating for improving the flowability of cohesive powders. *Powder Technol.* 2005;158:21–33.
18. Lu XS, Li H. Fluidization of $CaCO_3$ and Fe_2O_3 particle mixtures in a transverse rotating magnetic field. *Powder Technol.* 2000;107:66–78.
19. Hristov JY. Magnetic field assisted fluidization—a unified approach. Part 1: Fundamentals and relevant hydrodynamics. *Rev Chem Eng.* 2002;18:295–509.
20. Hristov JY. Magnetically assisted gas–solid fluidization in a tapered vessel. Part 1: Magnetization-LAST mode. *Particuology.* 2009;7:26–34.
21. Hristov JY. Magnetic field assisted fluidization—a unified approach. Part 3: Heat transfer in gas–solid fluidization beds—a critical re-evaluation of the results. *Rev Chem Eng.* 2003;19:229–355.
22. Rakoczy R. Hydro-thermal behavior of liquid systems in a magnetic field. Doctor's Thesis (in polish). West Pomeranian University of Technology, Szczecin, 2006.
23. Hristov JY. Magnetically assisted gas–solid fluidization in a tapered vessel: first report with observations and dimensional analysis. *Can J Chem Eng.* 2008;86:470–492.
24. Hristov JY. Magnetic field assisted fluidization—a unified approach. Part 5: Hydrodynamic treatise on liquid-solid fluidization beds. *Rev Chem Eng.* 2006;22:195–375.
25. Penchev P, Hristov JY. Fluidization of beds of ferromagnetic particles in a transverse magnetic field. *Powder Technol.* 1990;62:1–11.
26. Casal J, Amaldos J. The structure of magnetized-fluidized beds. *Powder Technol.* 1991;64:43–48.
27. Saxena C, Ganzha VL, Rahman SH, Dolidovich AF. Heat transfer and relevant characteristics of magnetofluidized beds. *Adv Heat Transfer.* 1994;25:151–249.
28. Hristov JY. Magnetic field assisted fluidization dimensional analysis addressing the physical basis. *China Particuology.* 2007;5:103–110.
29. Yo Q, Dave R, Zhu C, Quevedo J, Pfeffer R. Enhanced fluidization of nanoparticles in a oscillating magnetic field. *AICHE J.* 2005;51:1971–1979.
30. Hao Z, Zhu Q, Lei Z, Li H. CH_4-CO_2 reforming over Ni/Al_2O_3 aerogel catalysts in a fluidized bed reactor. *Powder Technol.* 2008;182:474–479.
31. Hao Z, Zhu Q, Jiang ZLH. Fluidization characteristics of aerogel Co/Al_2O_3 catalyst in a magnetic fluidized bed and its application to CH_4-CO_2 reforming. *Powder Technol.* 2008;183:46–52.
32. Hausmann R, Reichert C, Franzreb M, Höll WH. Liquid-phase mass transfer of magnetic ionexchangers in magnetically influences fluidized beds. *React Funct Polym.* 2004;60:17–26.
33. Reichert C, Hoell WH, Franzreb M. Mass transfer enhancement in stirred suspensions of magnetic particles by the use of alternating magnetic fields. *Powder Technol.* 2004;145:131–138.
34. Hartman H, Derksen JJ, van den Akker HEA. Numerical simulation of a dissolution process in a stirred tank reactor. *Chem Eng Sci.* 2006;61:3025–3032.
35. Kannan A, Pathan SK. Enhancement of solid dissolution process. *Chem Eng J.* 2004;102:45–49.
36. Nekrassov ZI, Chekin VV. The effect of an alternating magnetic field on a fluidized bed of ferromagnetic particles. Izvestiya Akademii Nauk SSSR. *Metallurgy Fuels.* 1961;6:25–29. (In Russian).
37. Nekrassov ZI, Chekin VV. The effective viscosity of a fluidized bed of polydisperse ferromagnetic solids in alternating magnetic field. Izvestiya Akademii Nauk SSSR. *Metallurgy Fuels.* 1962;1:56–59. (In Russian).
38. Sinitsyn AP, Gusakov AV, Davydkin IY, Davydjin VY, Protas OV. A hyperefficent process of enzymatic cellulose hydrolysis in the intensive mass transfer reactor. *Biotechnol Lett.* 1993;15:283–288.
39. Hristov J, Ivanova V. Magnetic field assisted bioreactors. *Recent Res Dev Ferement Bioeng.* 1999;2:41–94.

Manuscript received Mar. 19, 2009, and revision received Sept. 2, 2009.